

GSA Archive #### Reflection shot gathers from San Francisco Bay with 3D traveltimes fits

Fig. 1 - Model of the San Andreas fault shown in depth contours.

Fig. 2 - Model of the Hayward fault shown in depth contours.

Fig. 3 - 1995 cable deployment 1 shot and receiver locations. The number labels correspond with gathers shown in Figs. 4-10.

Figs. 4-10. Shot gathers are shown from 1995 cable deployment 1 with modeled travel times superimposed. *These and all following gathers shown are not necessarily the highest quality data, but were chosen to span the geographic extent of the coverage.* To generate the traveltimes curves the finite-difference algorithm of Vidale (1990) is extended to compute reflection travel times (Hole and Zelt, 1995). The technique was developed for use in three dimensions; the reflector positions are projected onto a plane for display. The reflecting interface is defined as a sampled function of the horizontal coordinate, and is allowed to vary smoothly in depth. To begin the procedure, first arrival travel times are computed from the point source to the reflecting interface. Velocities below the reflector are defined to be equal to, or less than, velocities above in order to prevent waves transmitted through the interface from arriving as first arrivals at the reflector. The computed times at the reflecting interface are thus the times of the incident down-going wave. To allow a smooth reflector to exist between grid nodes in depth, the computed incident times at the grid nodes immediately above the reflector are used to analytically compute reflected times at the same nodes. Travel times to shallower grid nodes are replaced with large dummy values. This sampled travel time field is input into the finite-difference algorithm and travel times are computed upward from the base of the model. Previously computed times (in particular the large dummy values) are replaced by upgoing times if the upgoing times are earlier. In this manner, the incident travel times on the reflecting interface are used as a source to propagate the reflected wave upwards through the model.

Fig. 11 - 1995 cable deployment 2 shot and receiver locations. The number labels correspond with gathers shown in Figs. 12-15.

Figs. 12-15. Shot gathers are shown from 1995 cable deployment 2 with modeled travel times superimposed.

Fig. 16 - 1997 cable deployment 3 shot and receiver locations. The number labels correspond with gathers shown in Figs. 17-26.

Figs. 17-26. Shot gathers are shown from 1997 cable deployment 3 with modeled travel times superimposed.

Fig. 27 - 1997 cable deployment 4 shot and receiver locations. The number labels correspond with gathers shown in Figs. 28-38.

Figs. 28-38. Shot gathers are shown from 1997 cable deployment 4 with modeled travel times superimposed.

Fig. 39. Locations of 1995 land shots on San Francisco Peninsula shown in Figs. 40-44 and tectonic setting of the San Francisco Bay region. Much of the plate boundary slip is accommodated by right-lateral motion on the San Andreas, Hayward, and Calaveras faults. The Salinian terrane is separated from the Franciscan terrane by the Pilarcitos fault on San Francisco Peninsula. The shot points (sp) are marked with an asterisk (*) and the receiver array is indicated by the northeast trending gray line.

Figs. 40-44. Shot gathers are shown from 1995 land deployment with modeled travel times superimposed.

REFERENCE CITED

Vidale, J. E., 1990, Finite-difference calculation of traveltimes in three dimensions: Geophysics, v. 55, p. 521-526.

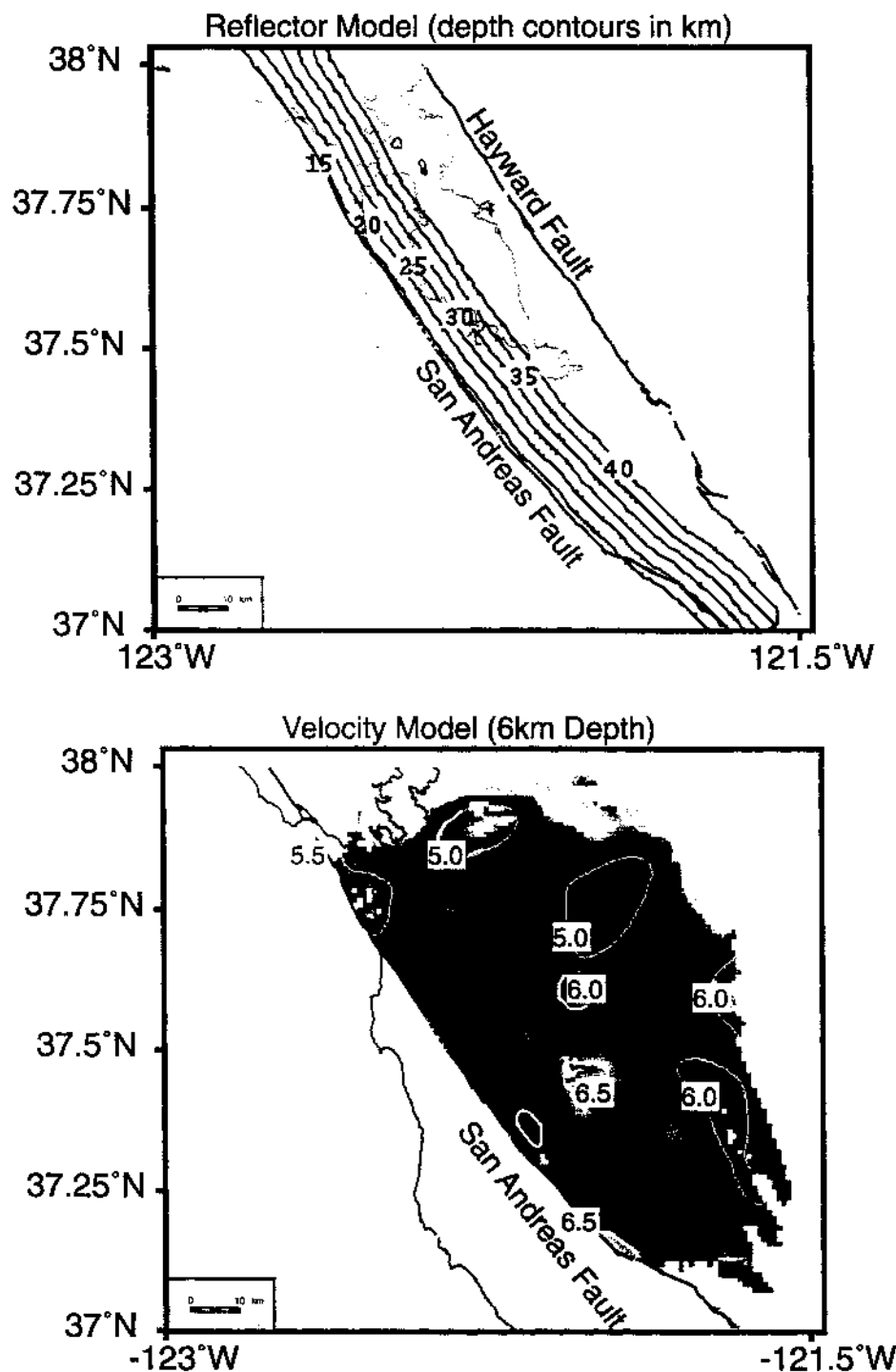


Figure 1

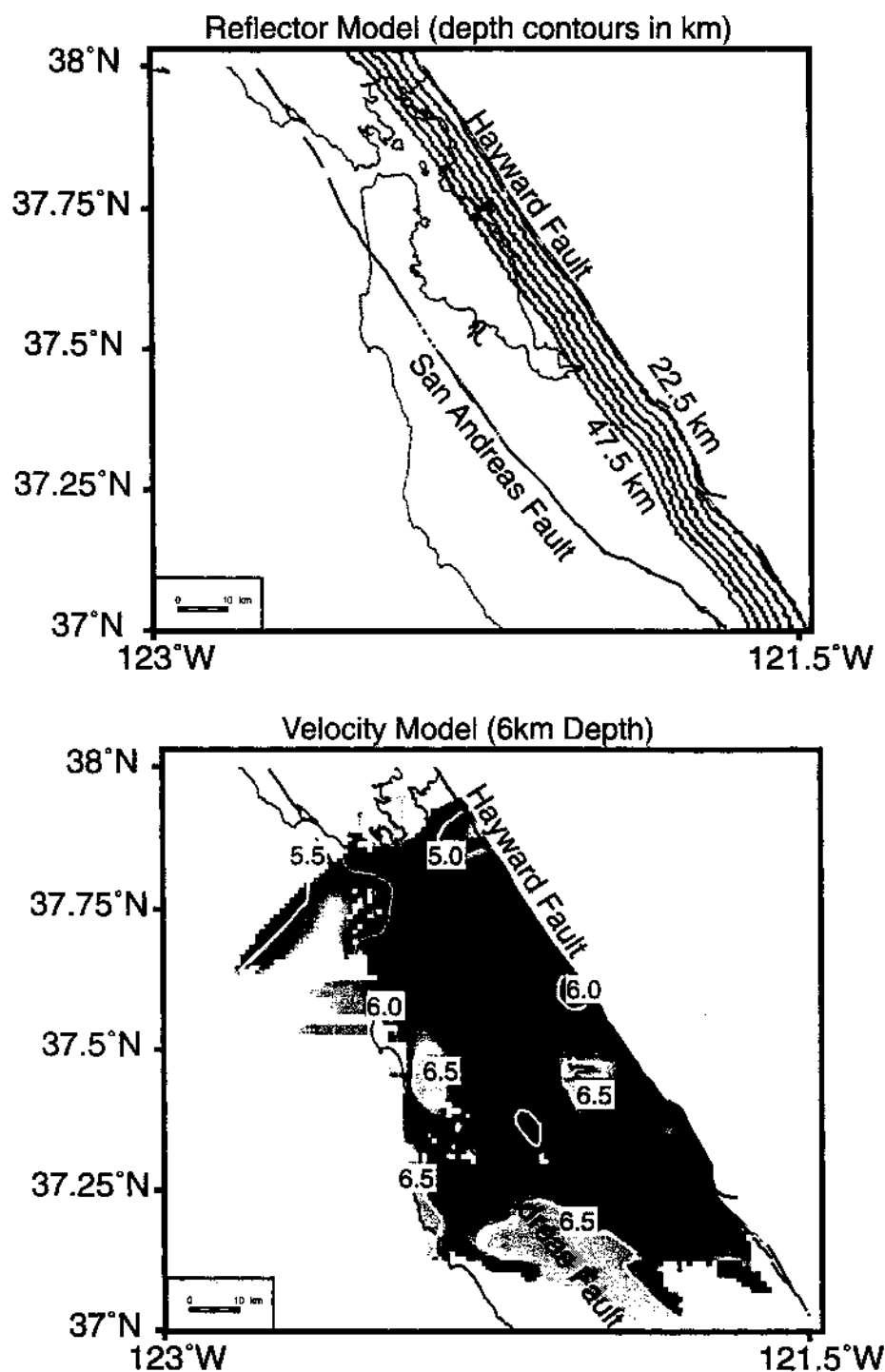


Figure 2

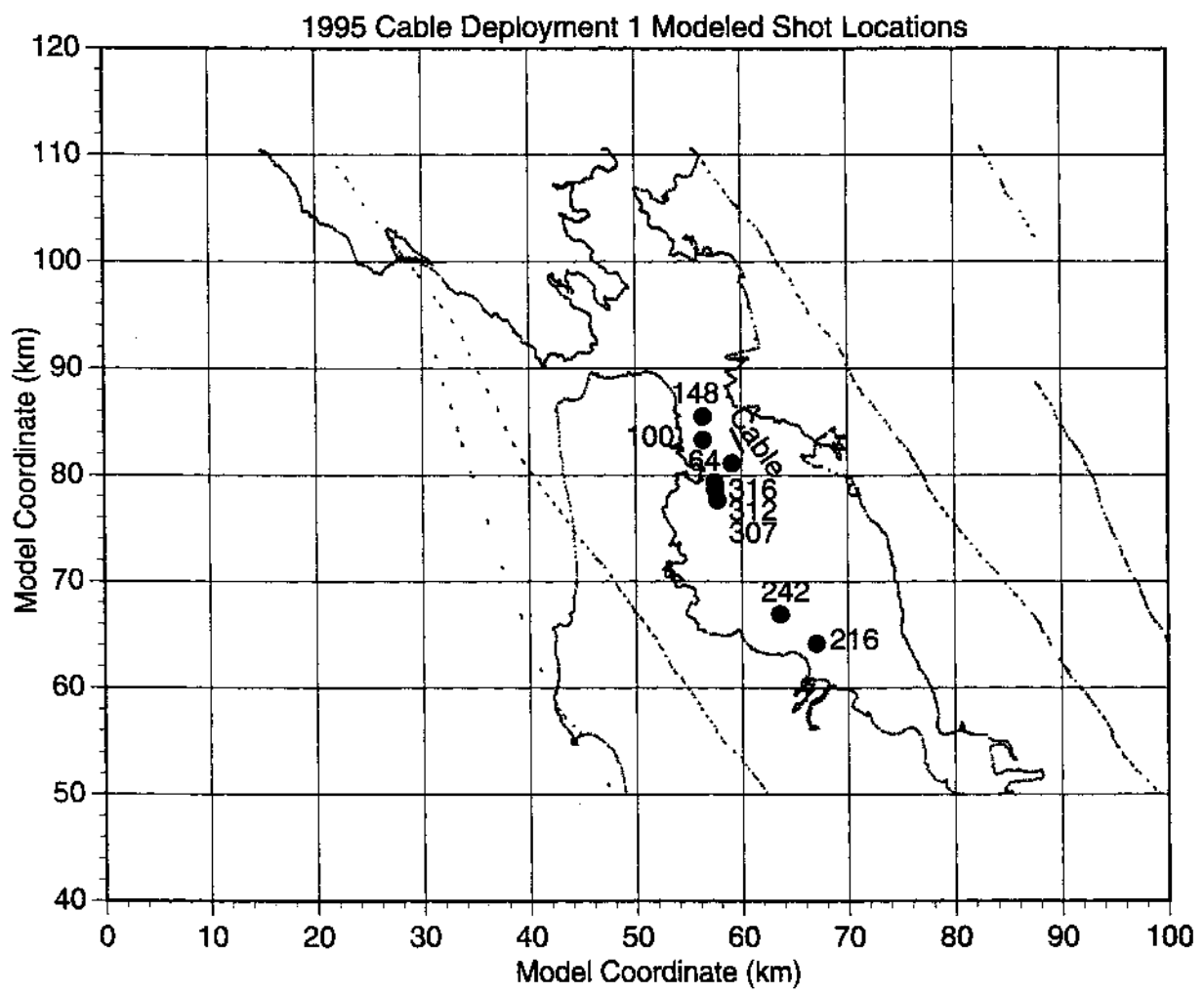


Figure 3

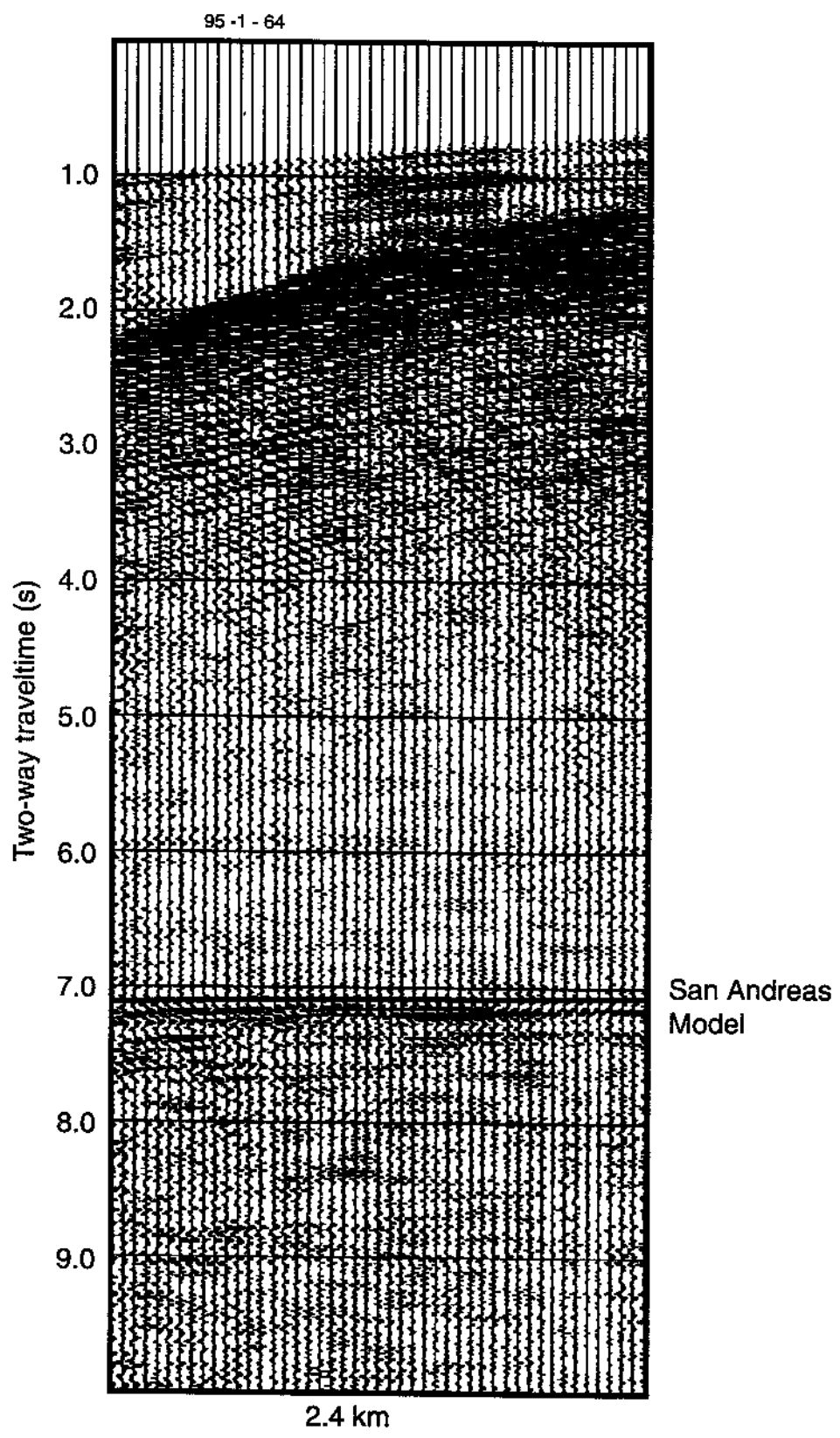


Figure 4

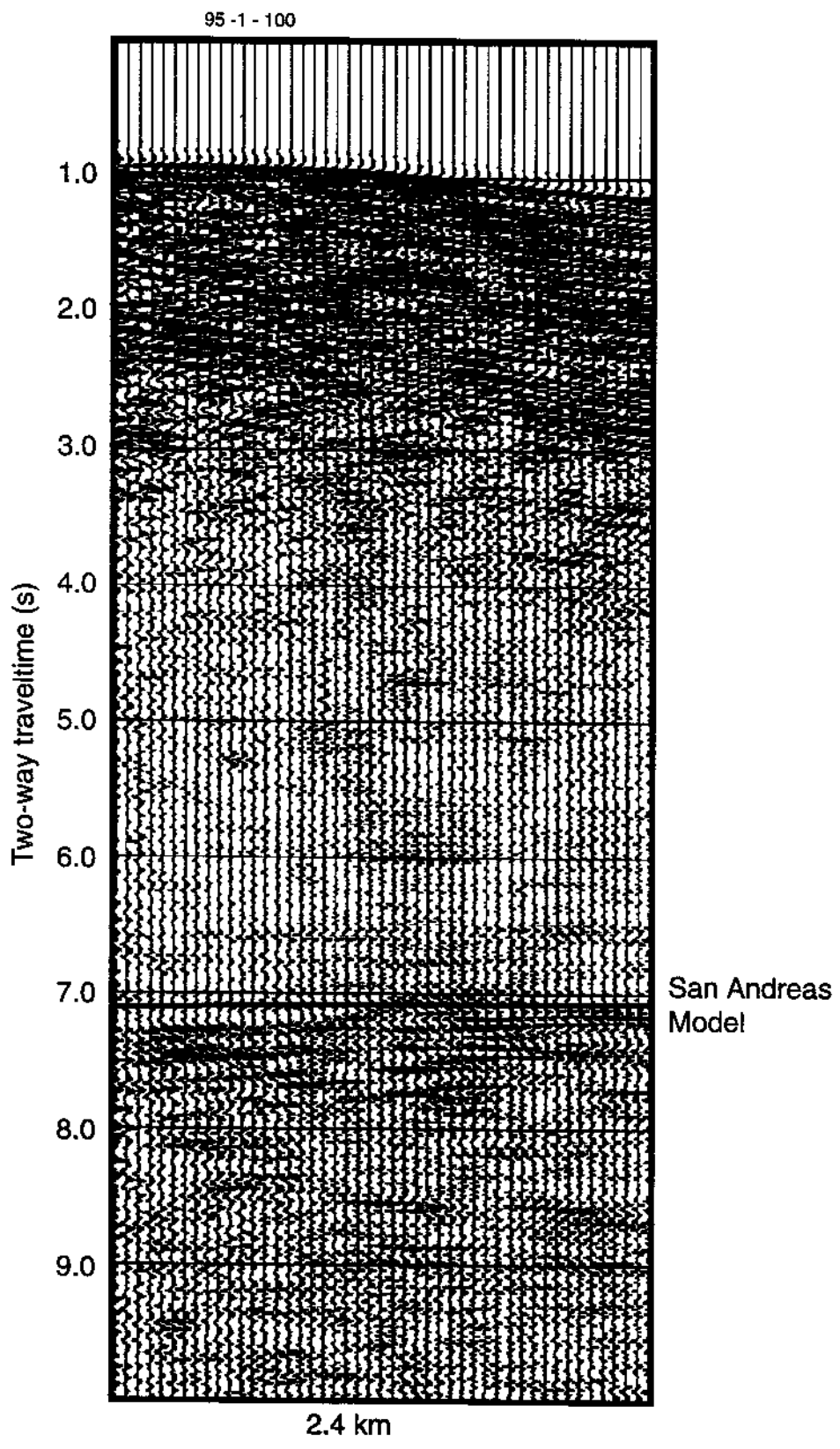


Figure 5

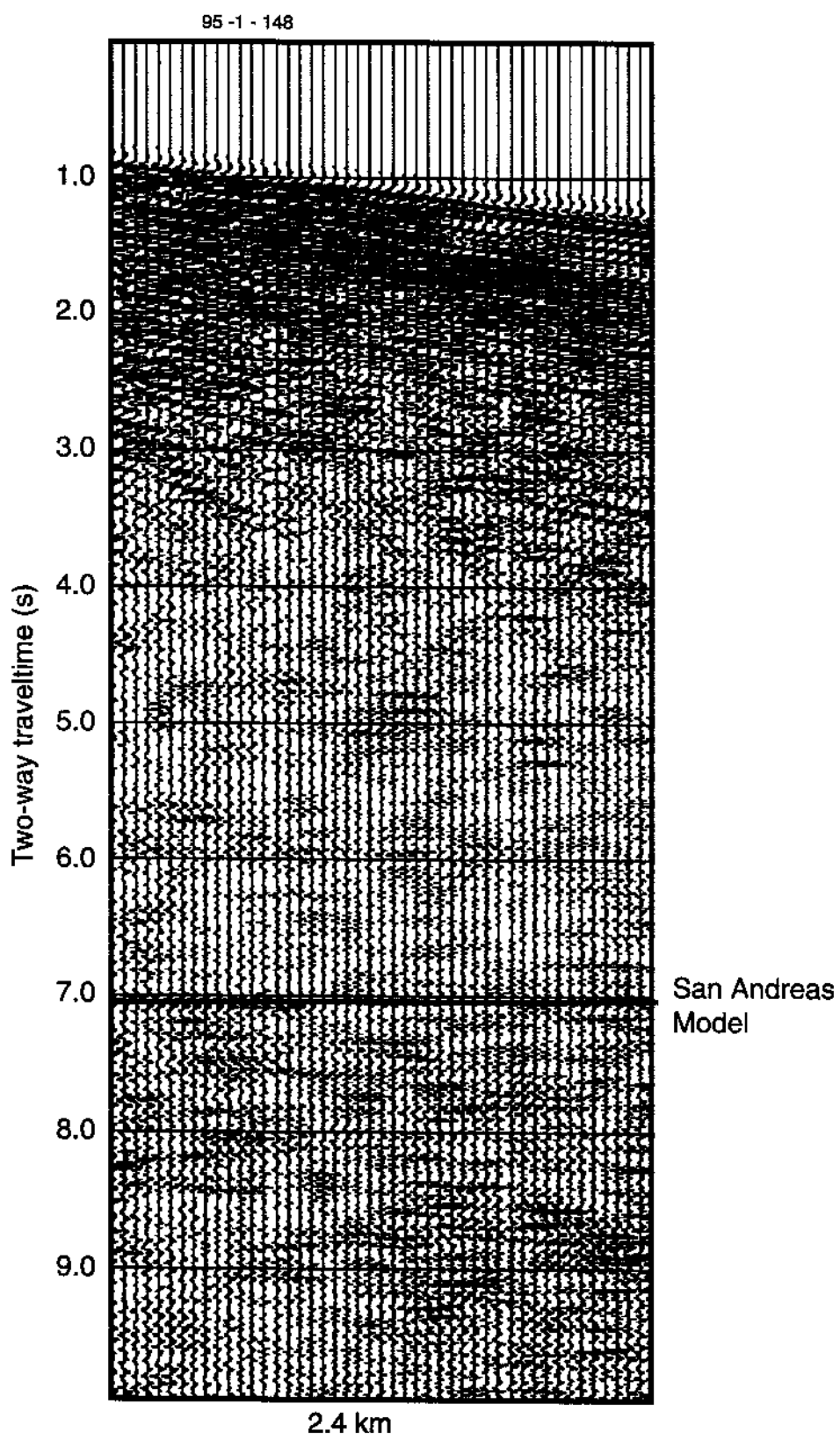


Figure 6

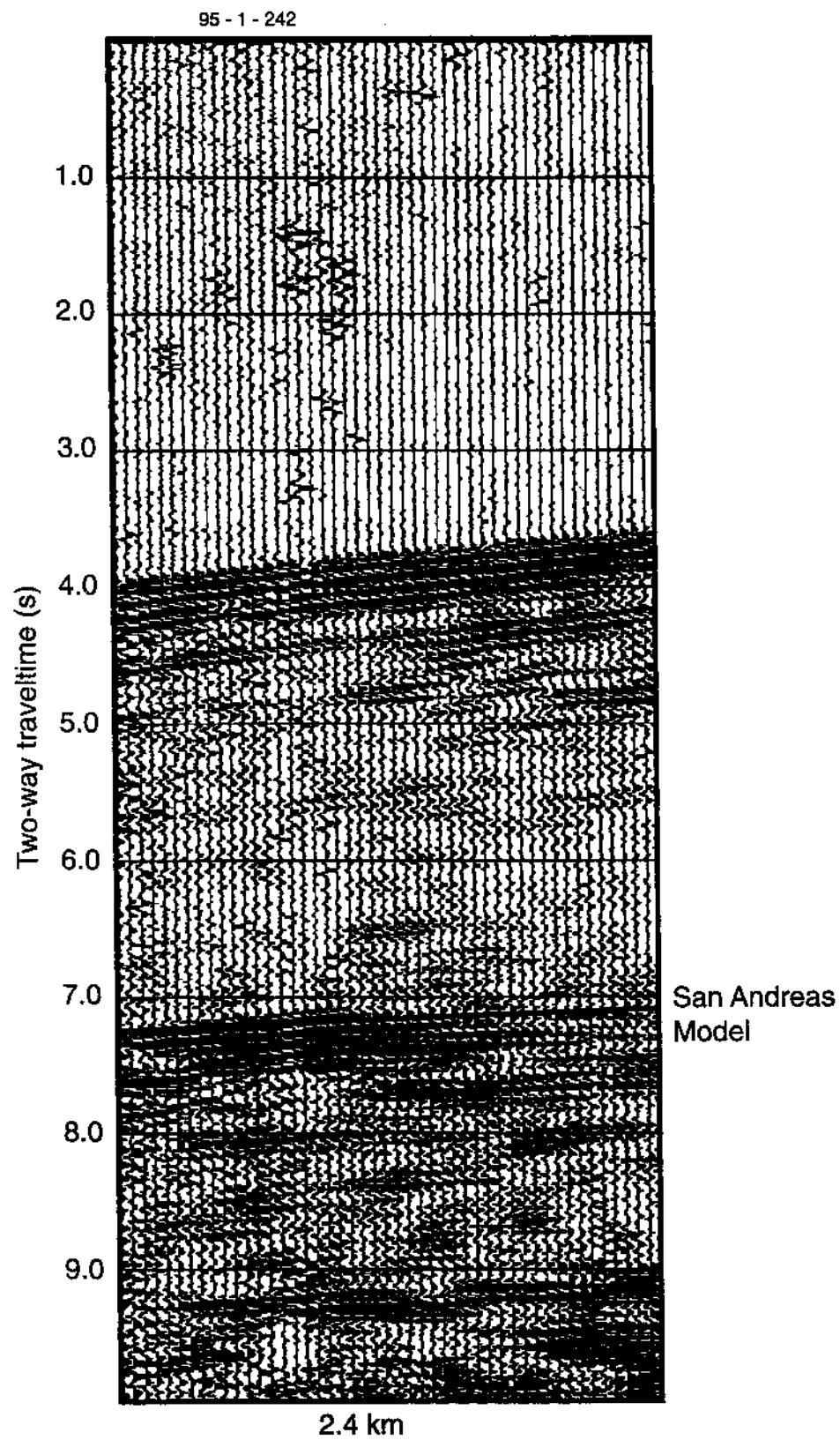


Figure 7

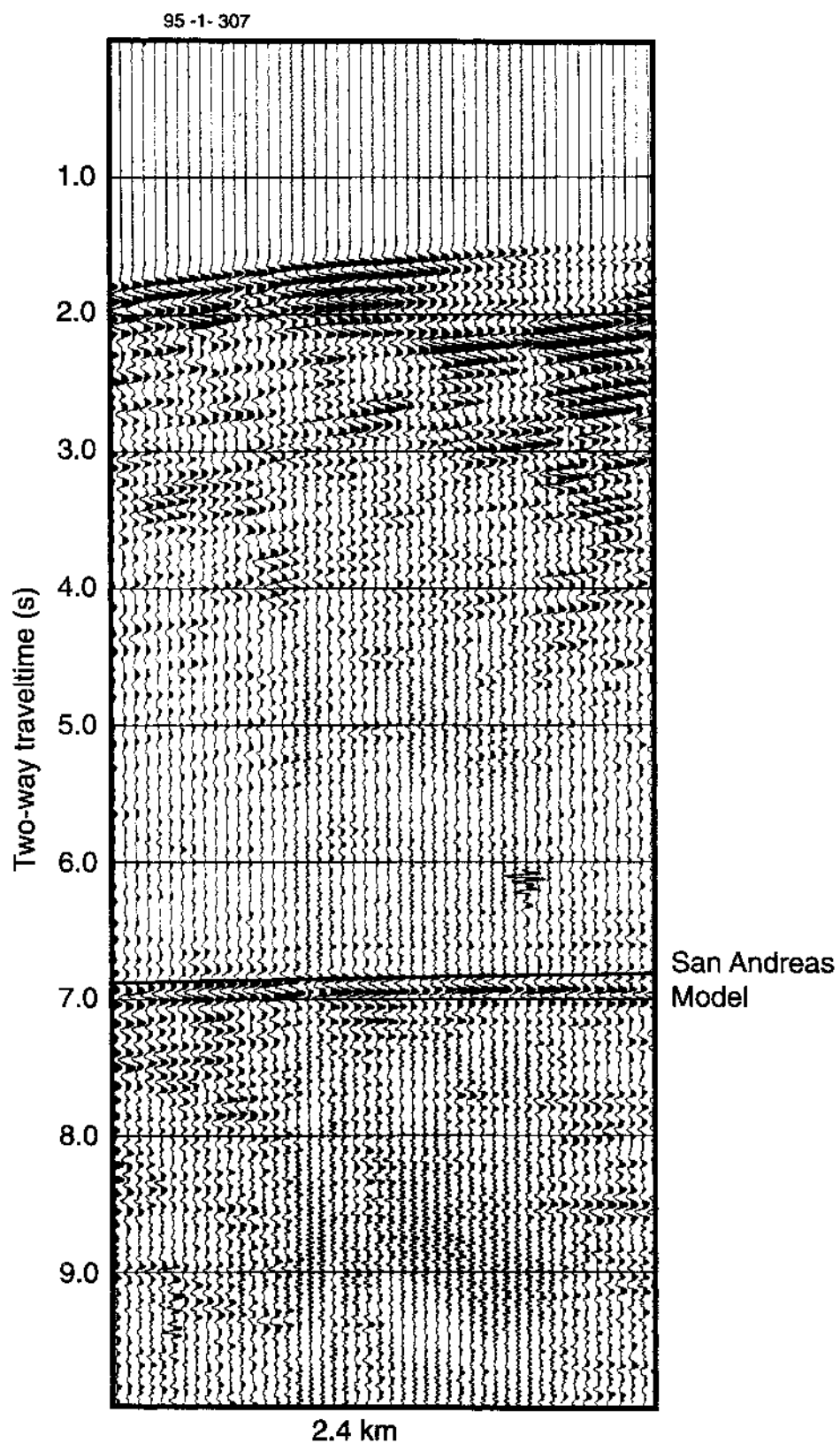


Figure 8

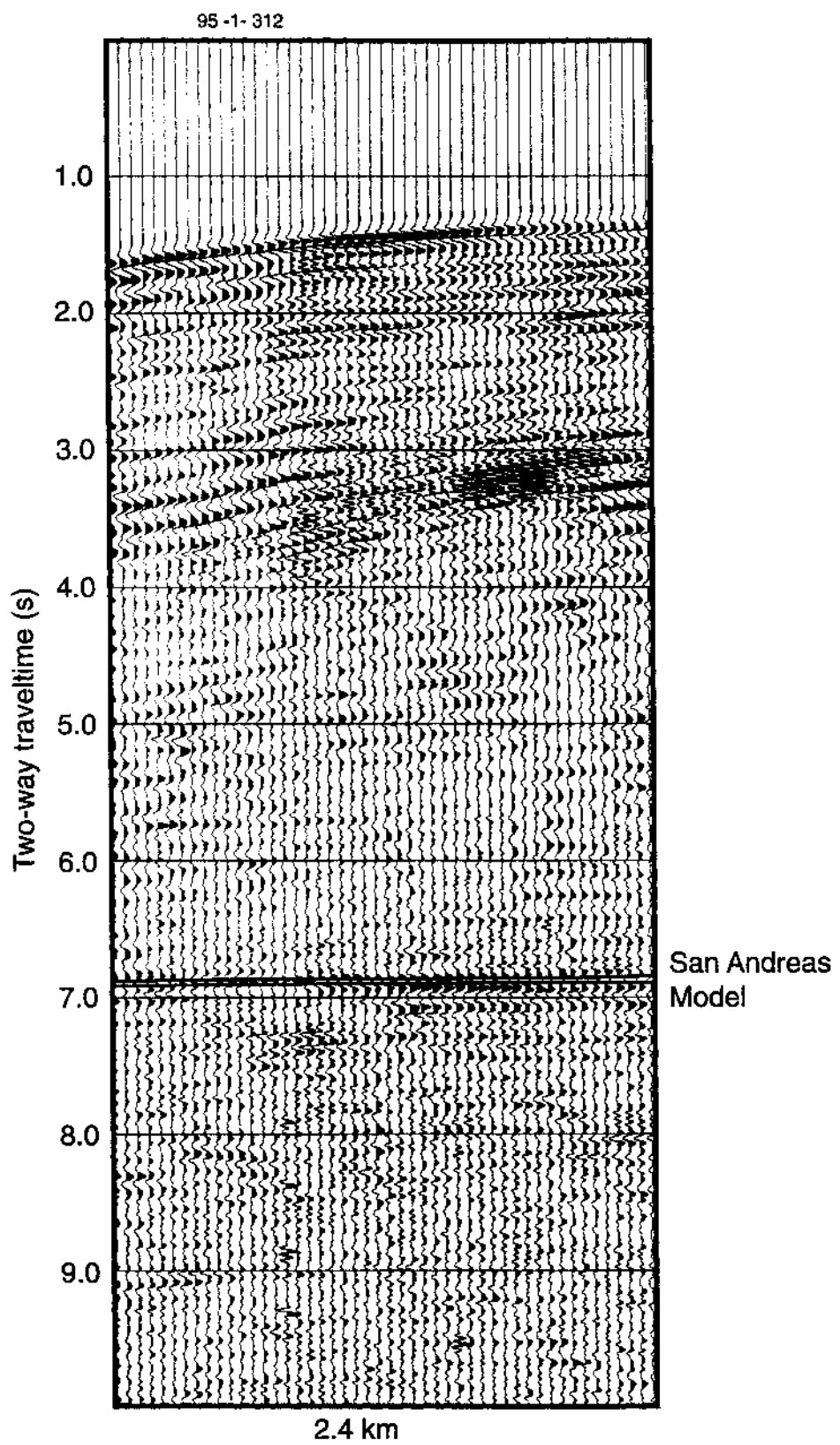


Figure 9

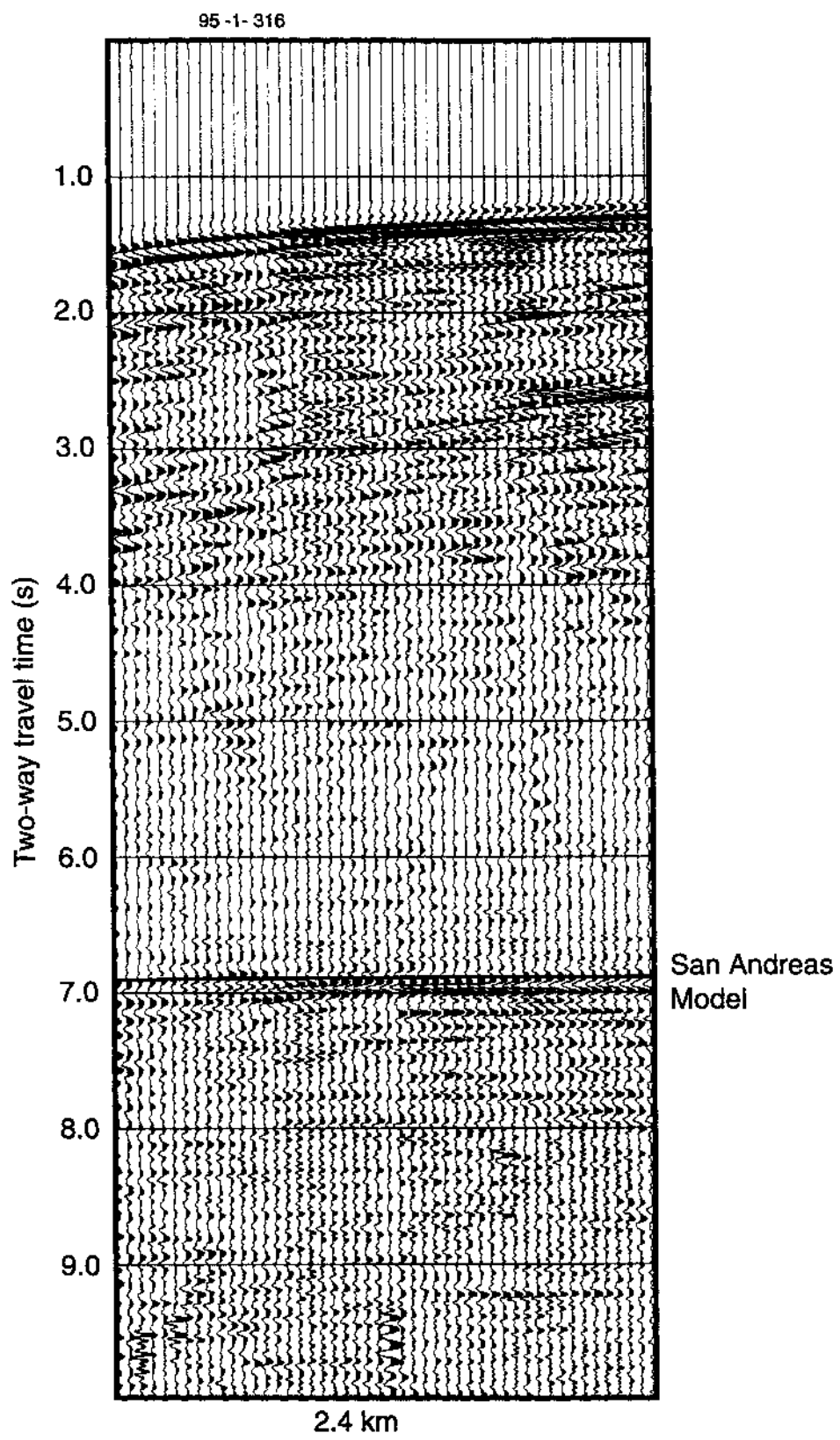


Figure 10

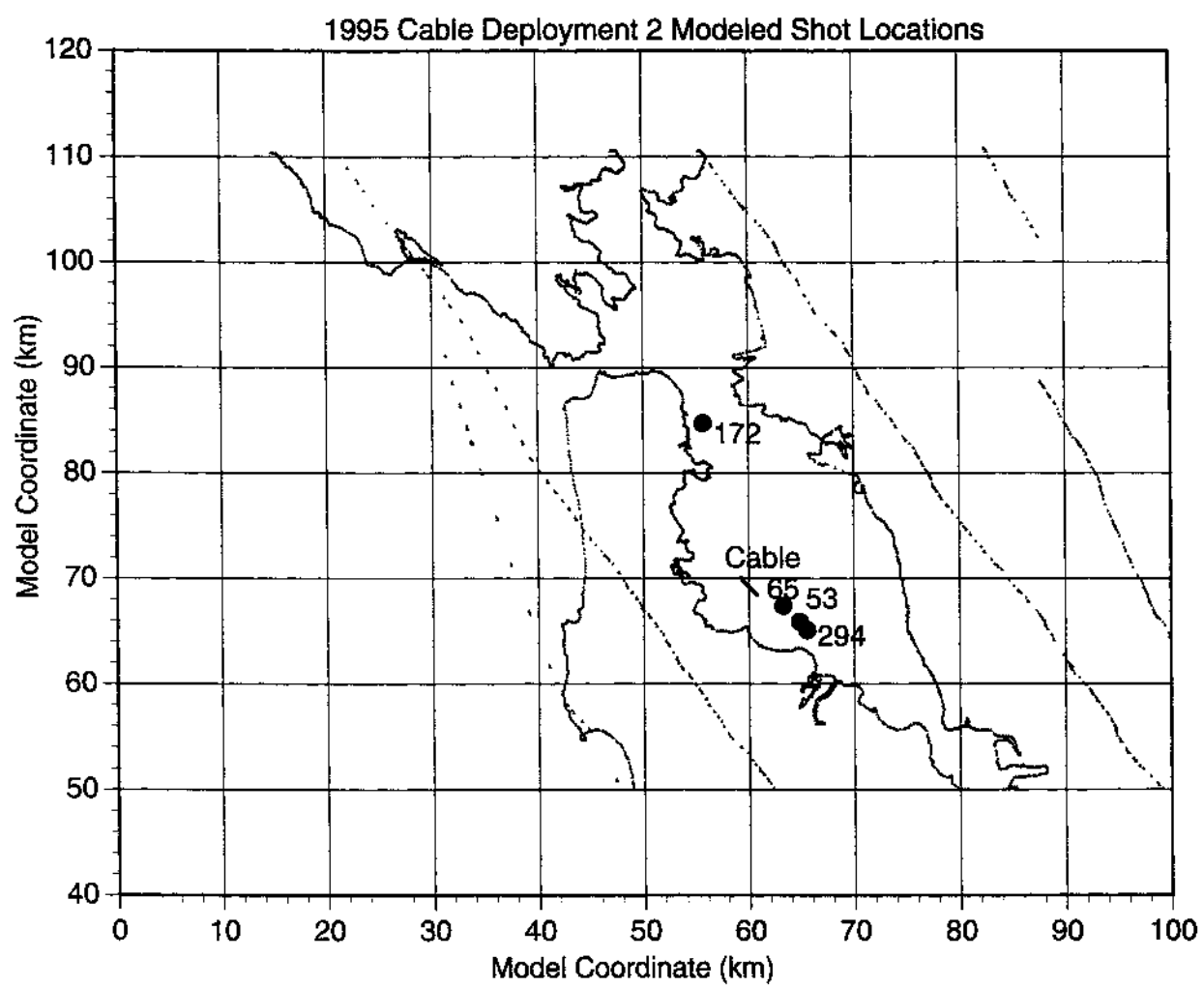


Figure 11

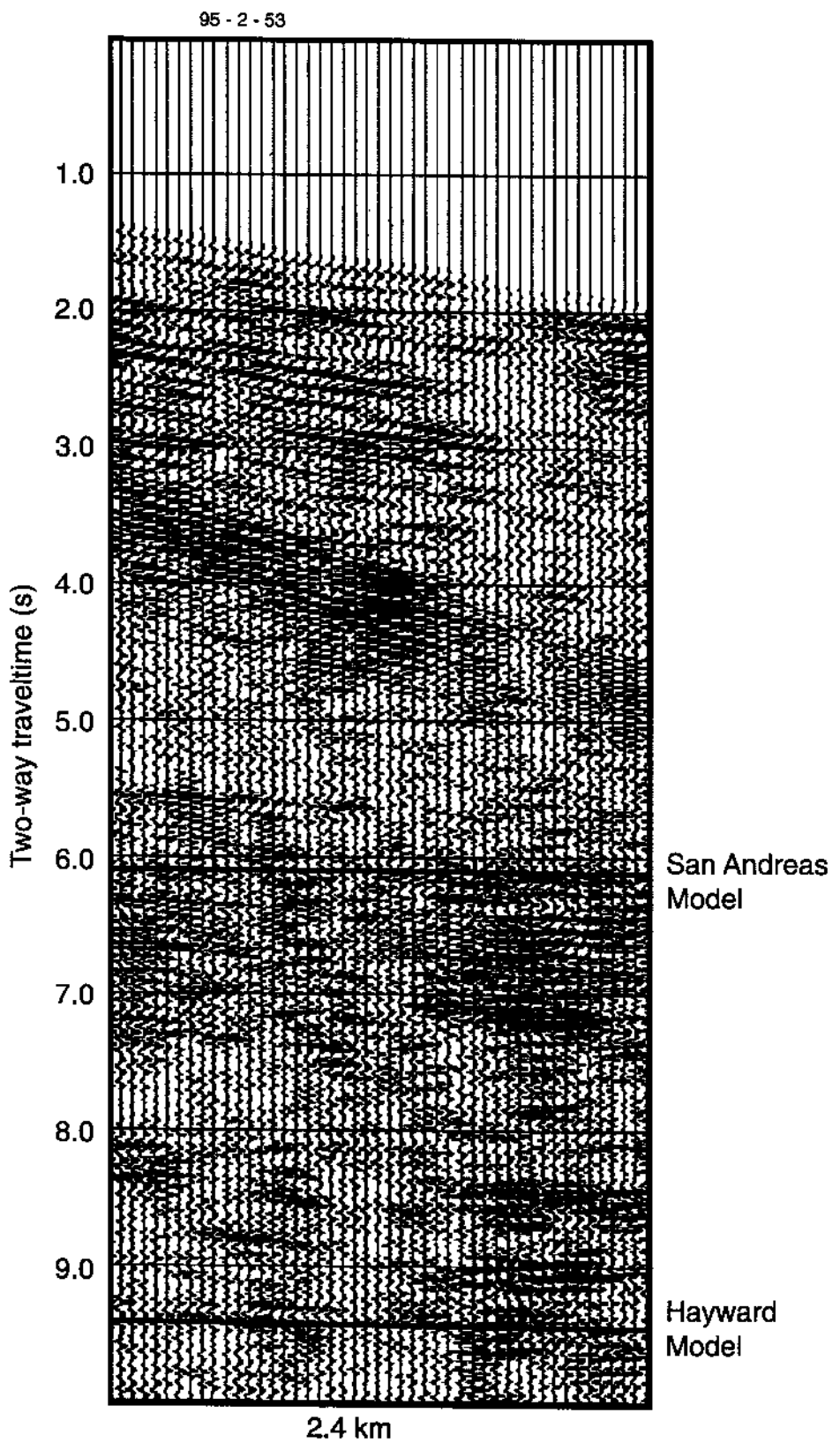


Figure 12

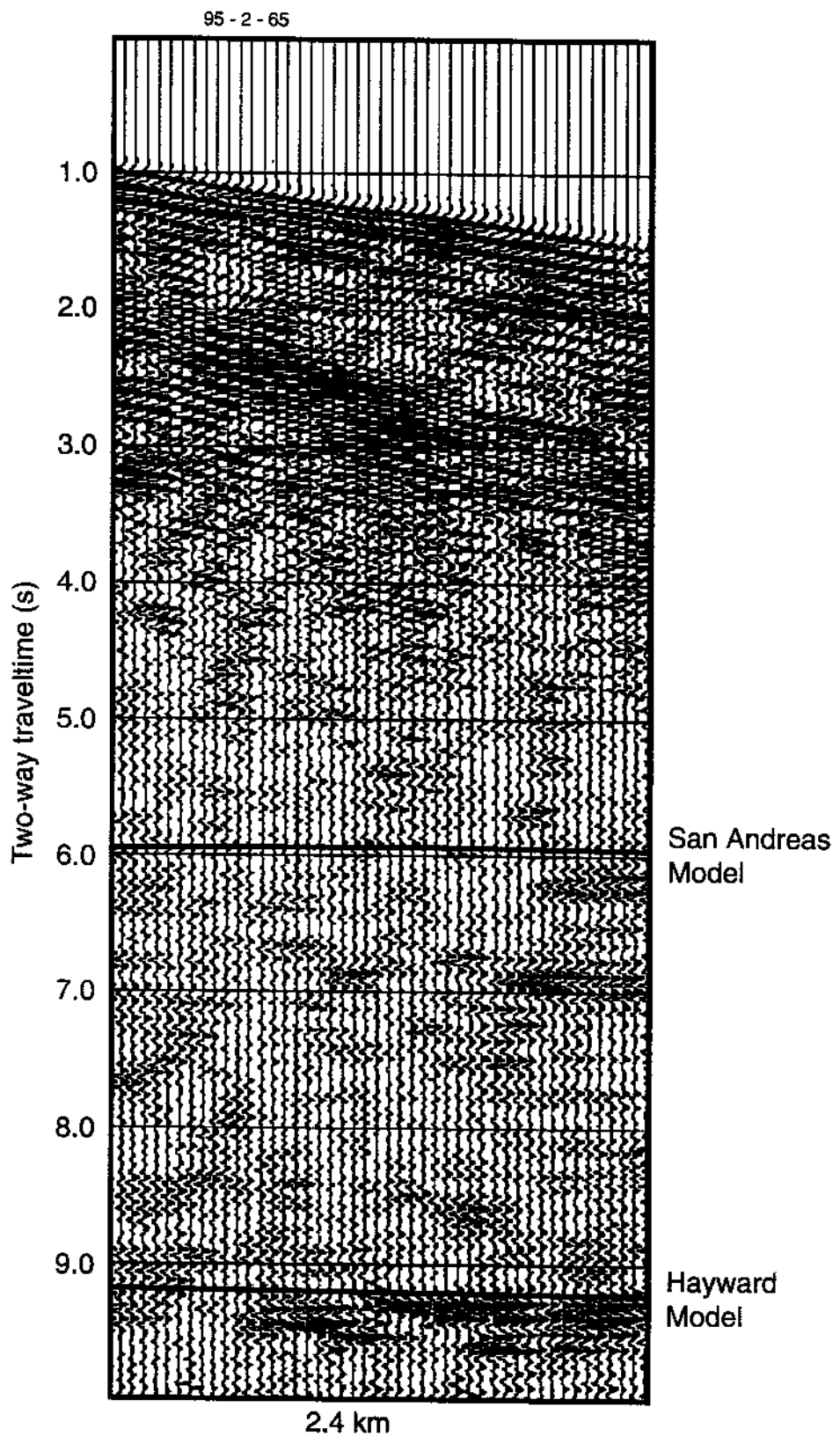


Figure 13

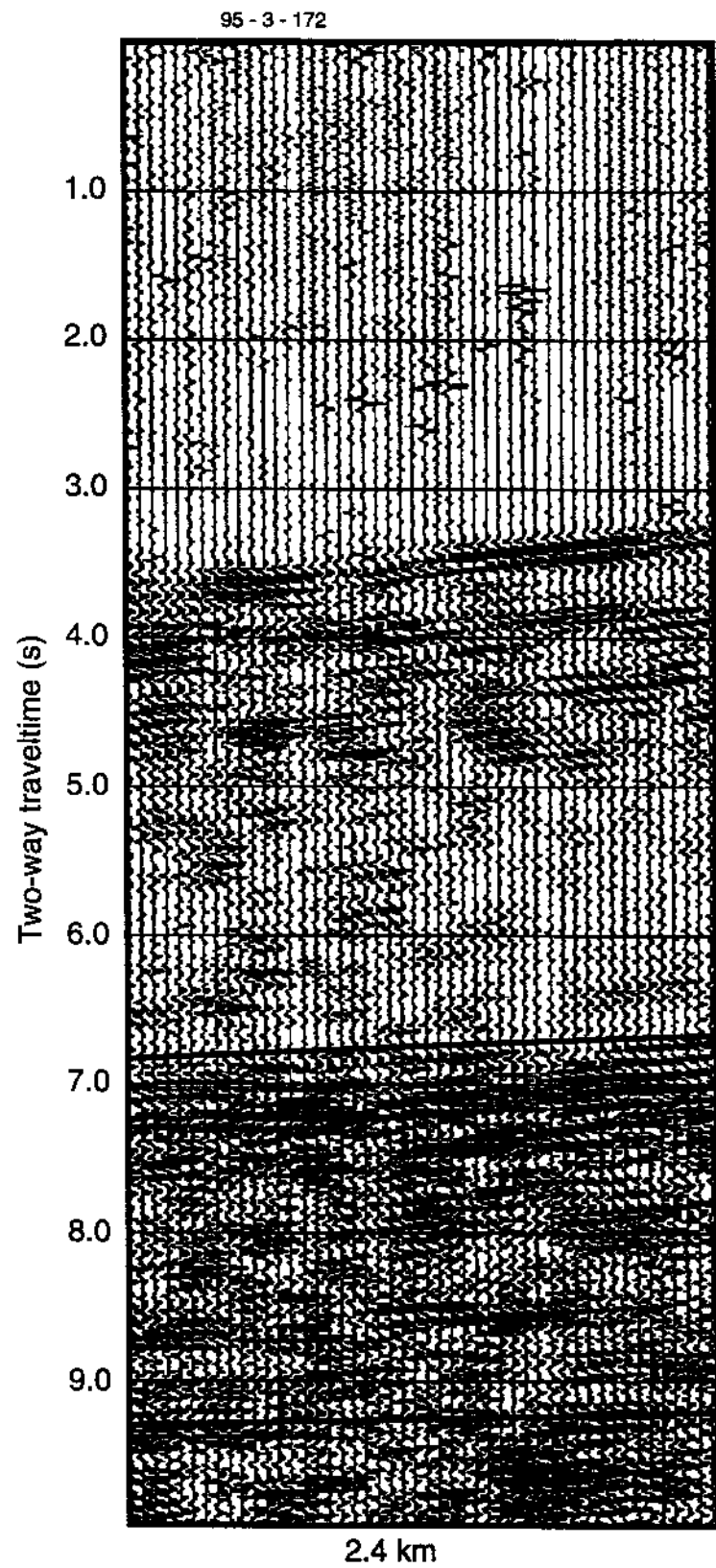


Figure 14

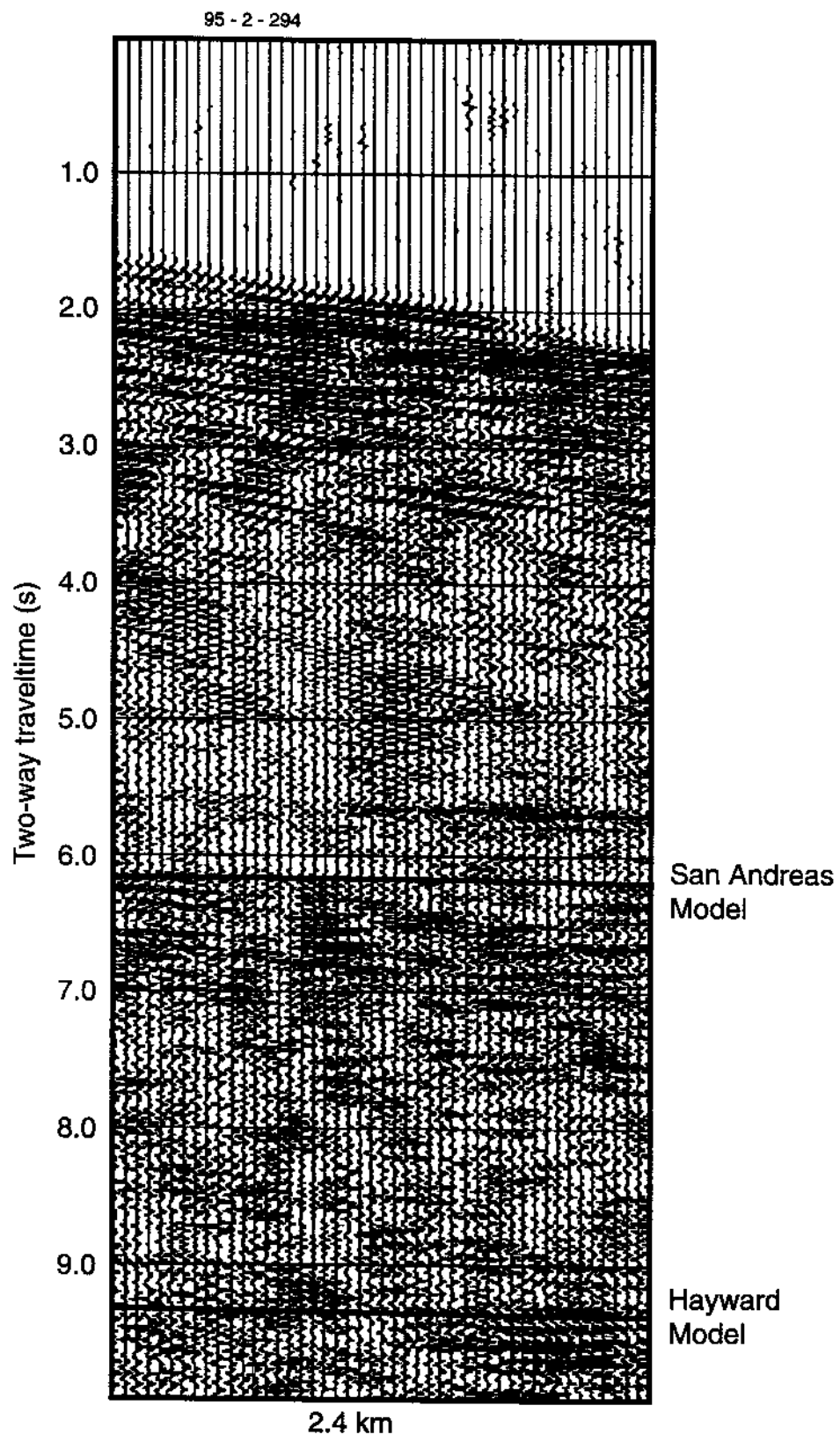


Figure 15

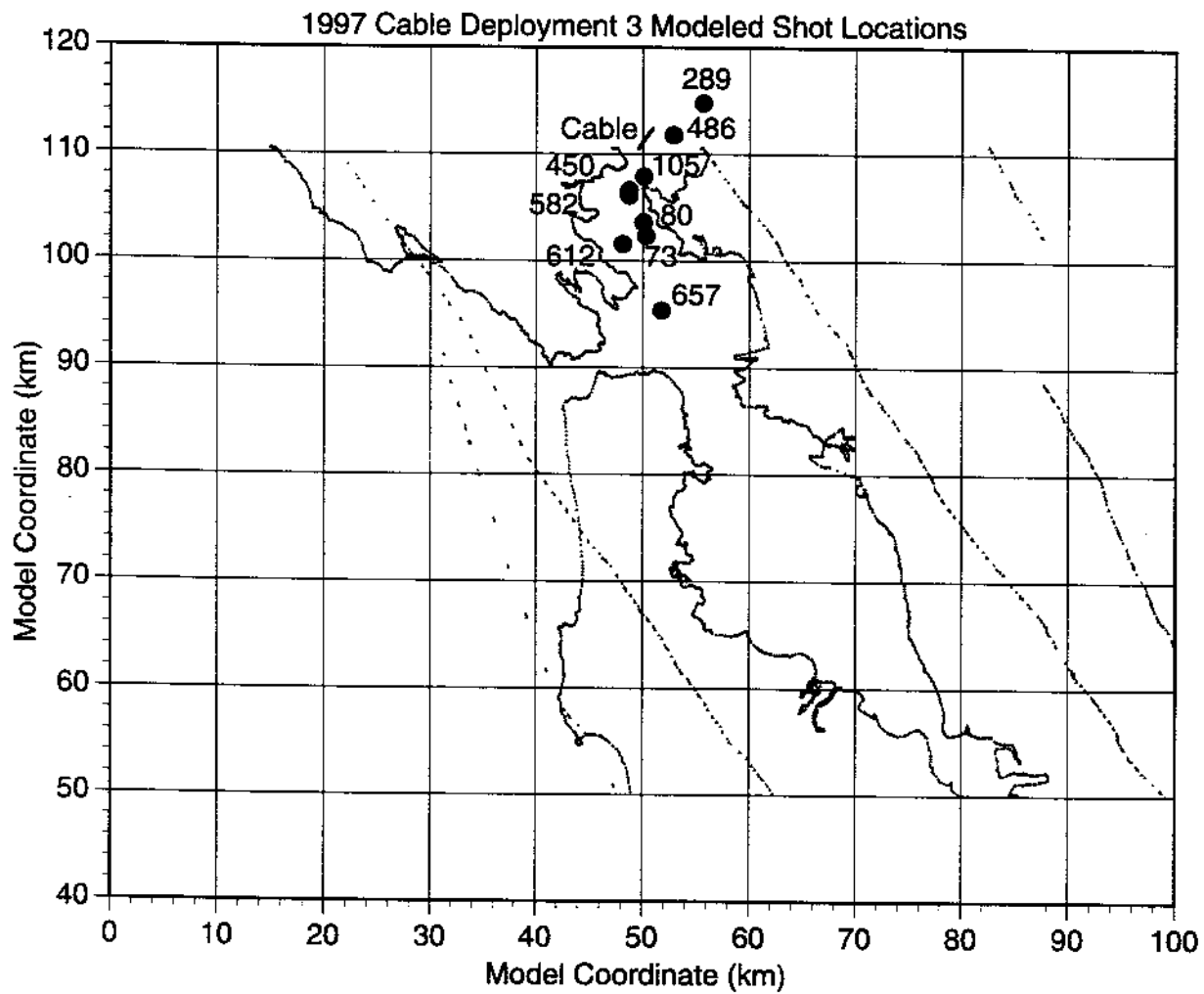


Figure 16

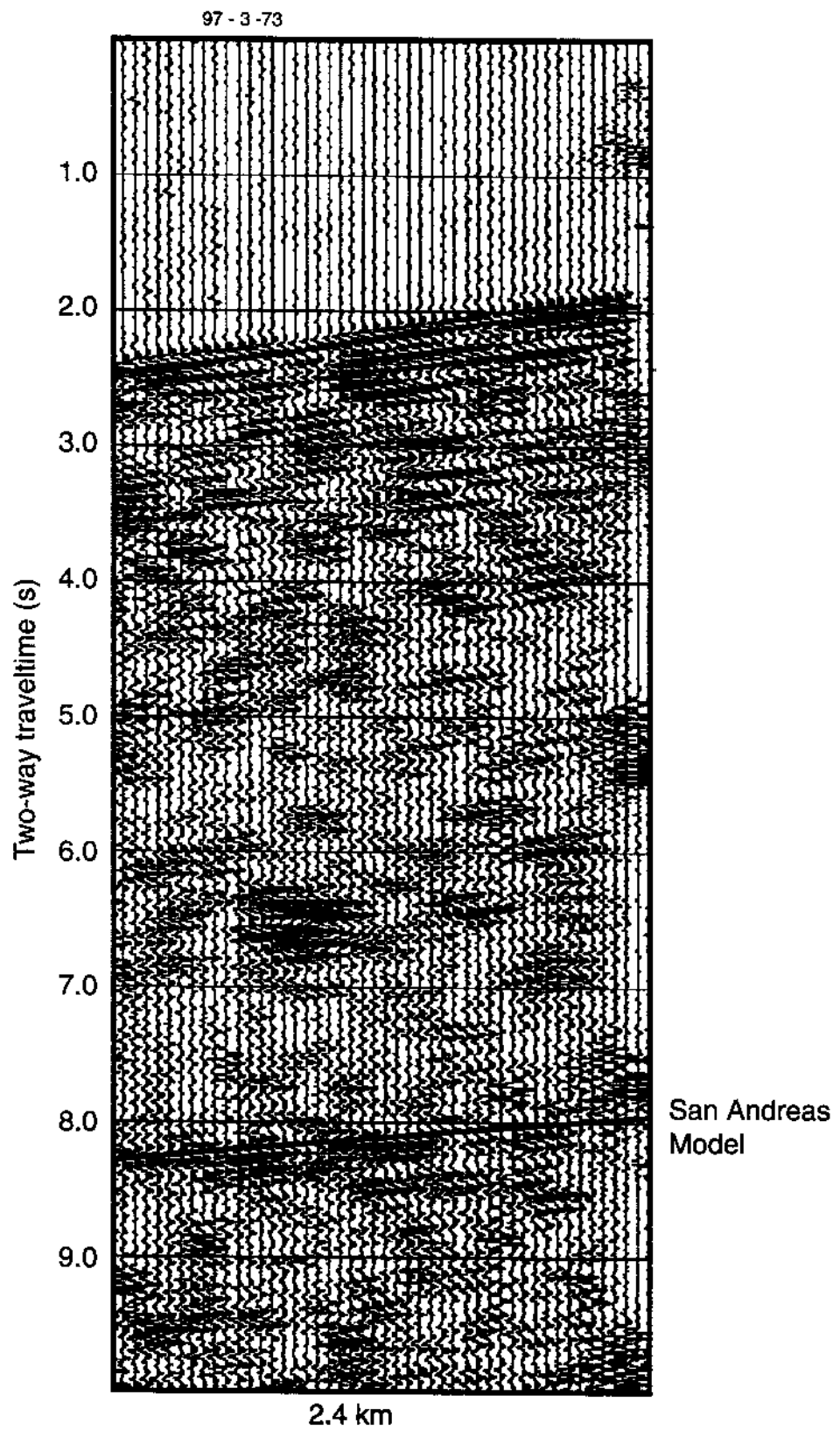


Figure 17

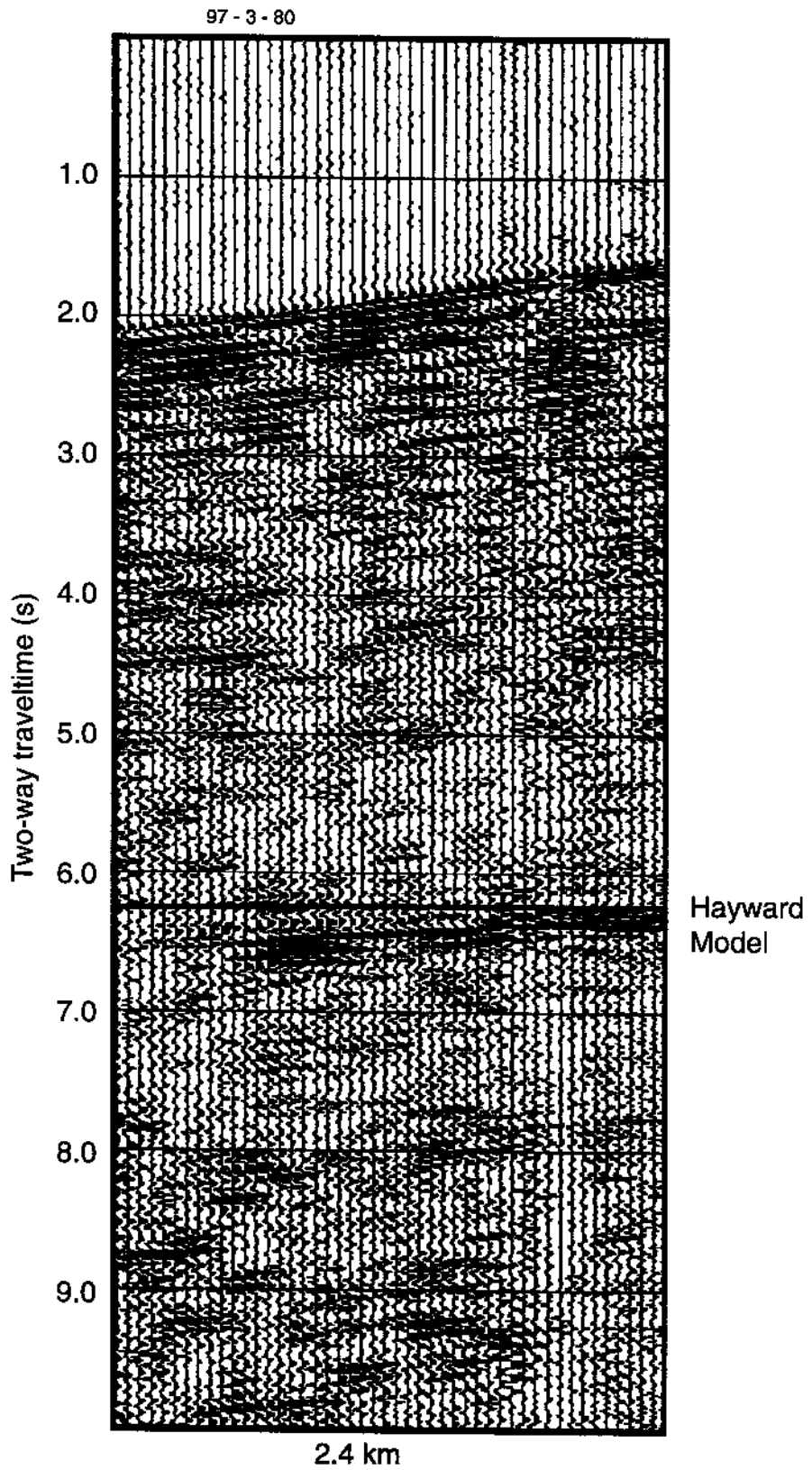


Figure 18

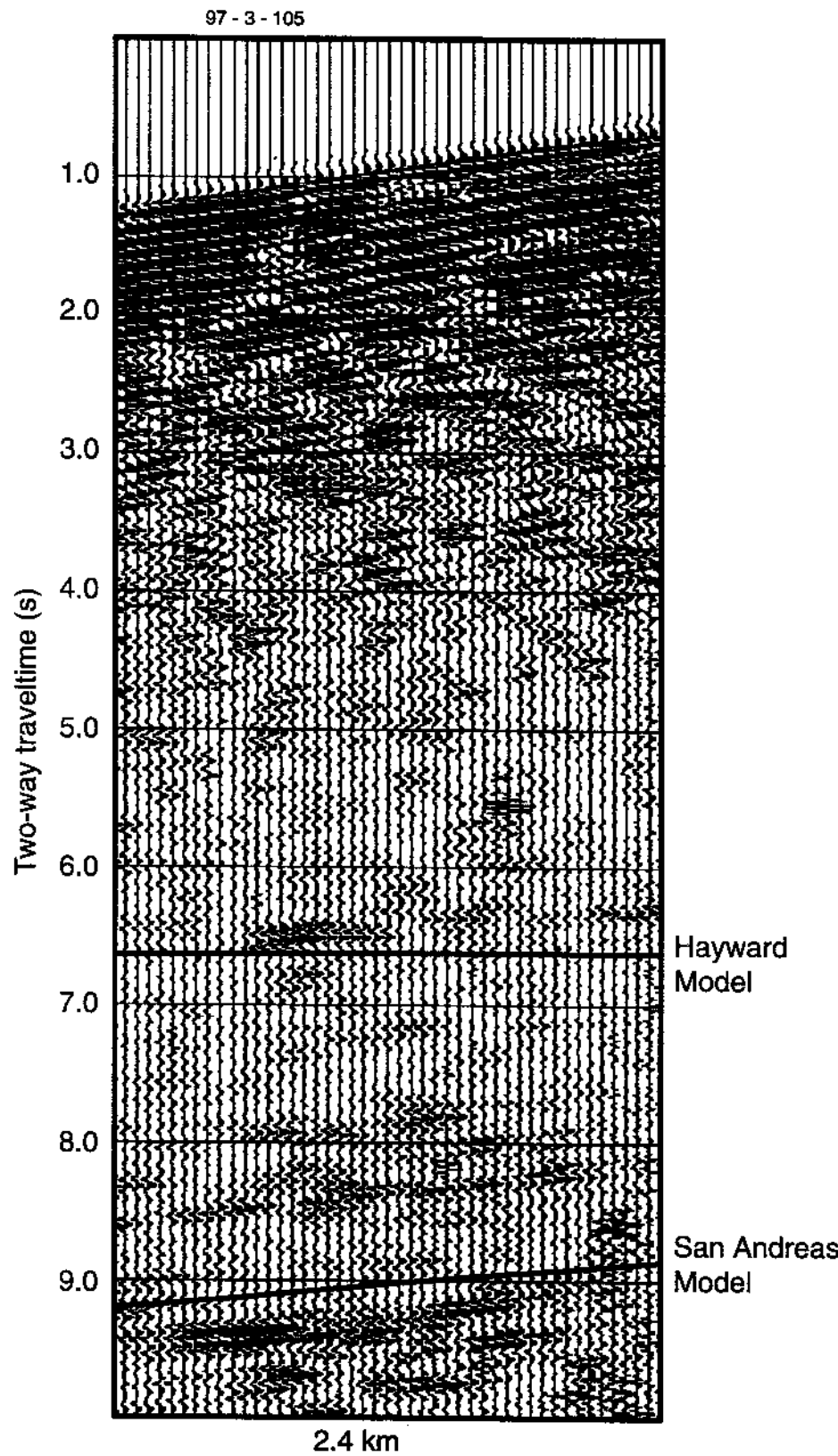


Figure 19

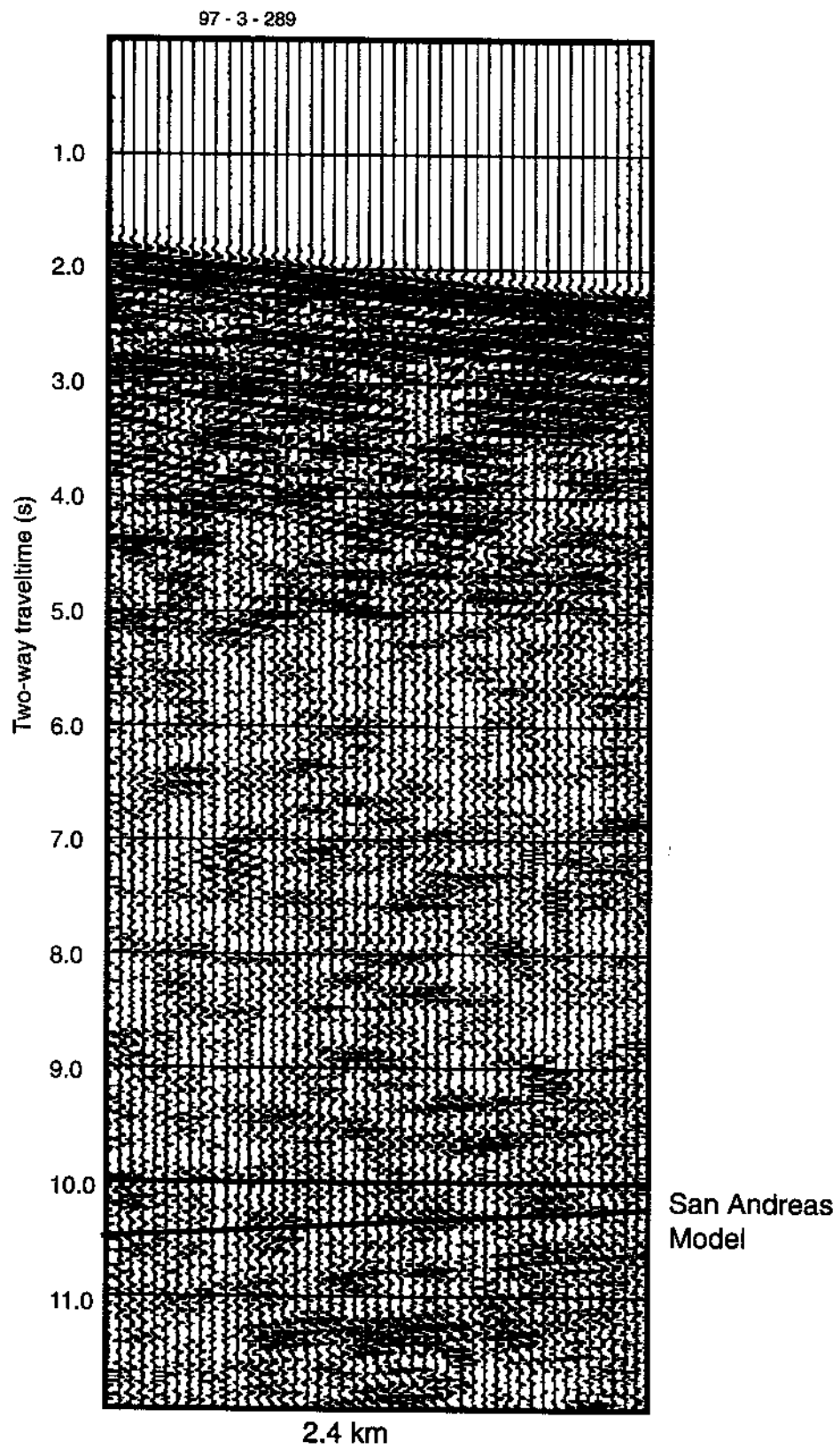


Figure 20

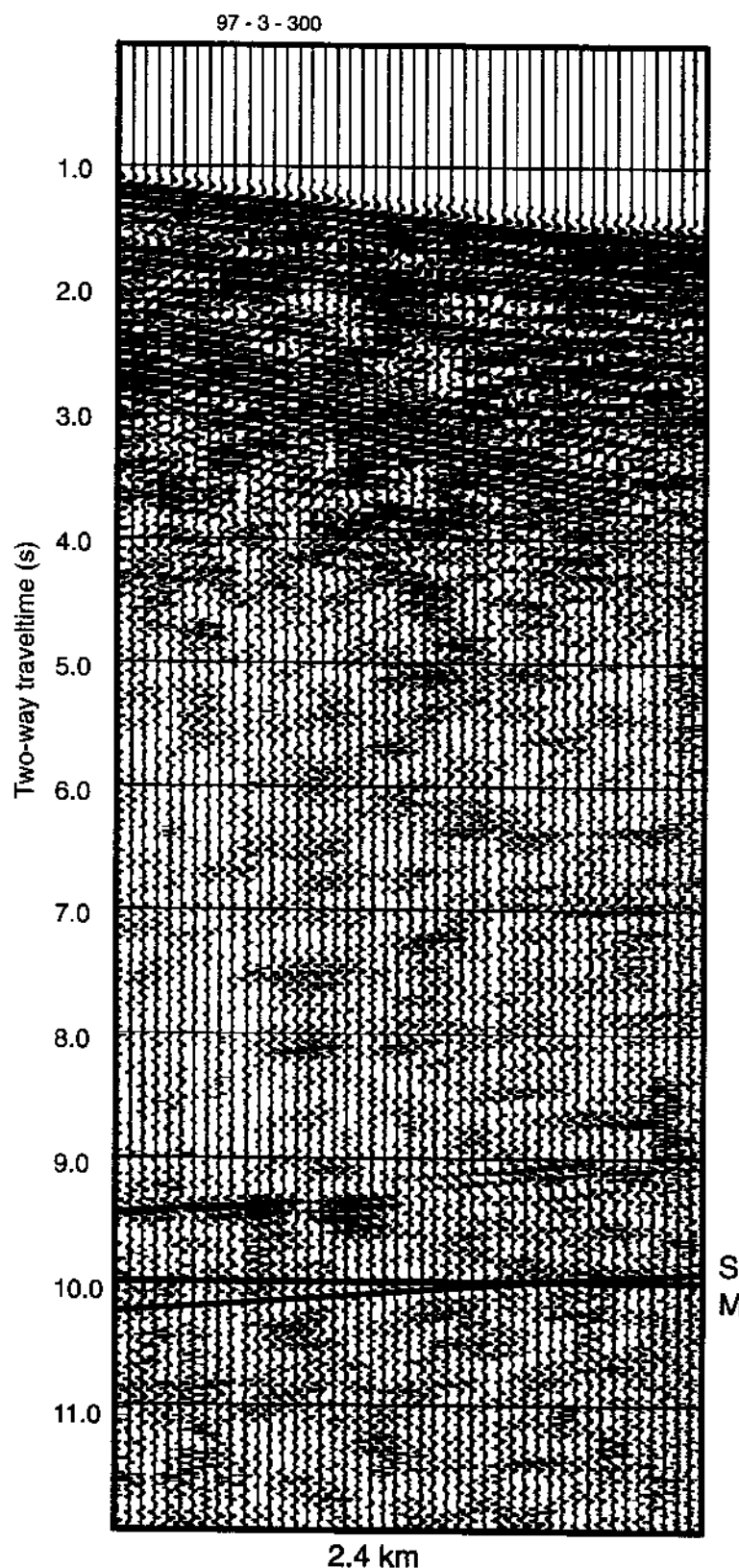


Figure 21

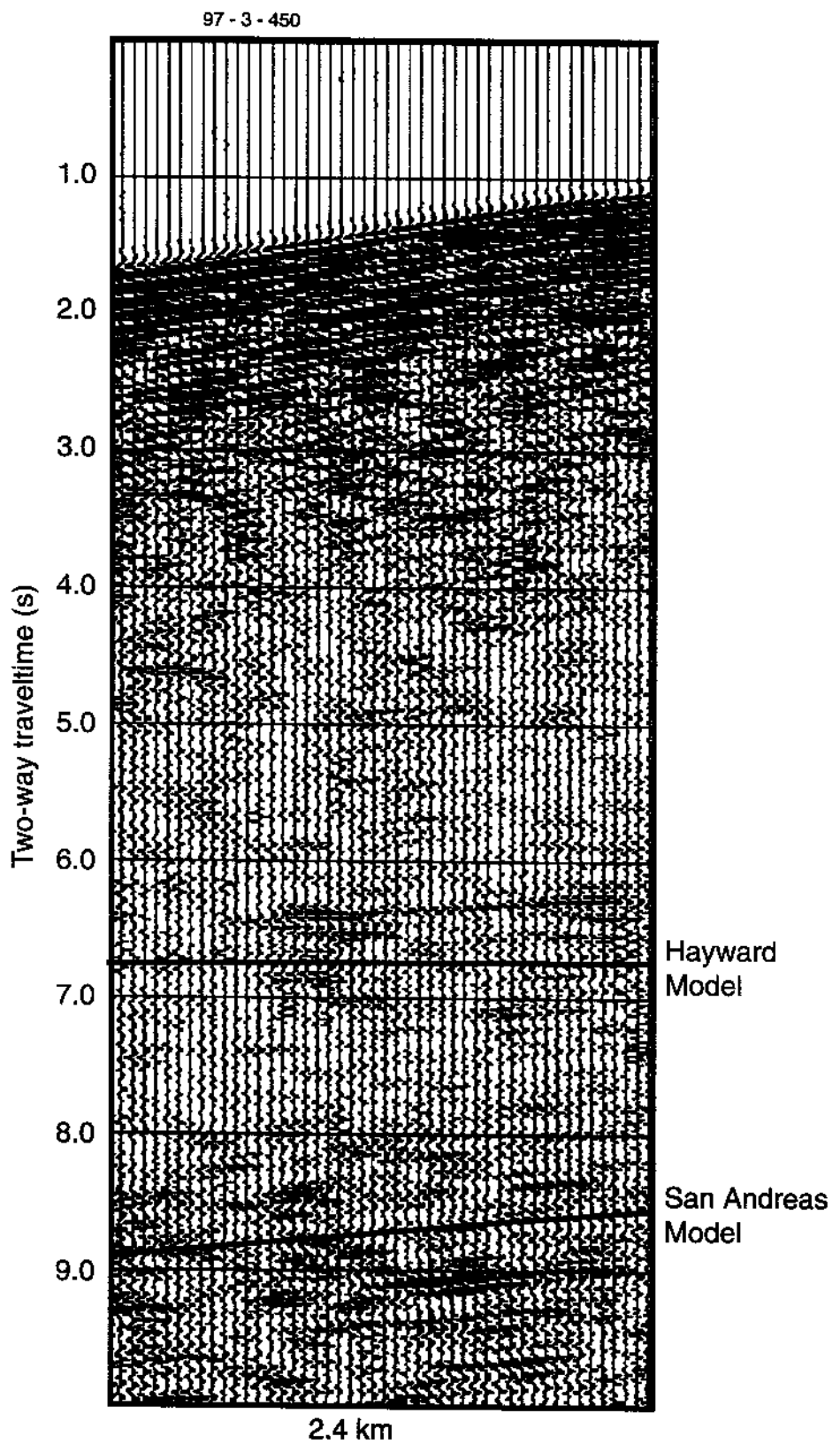


Figure 22

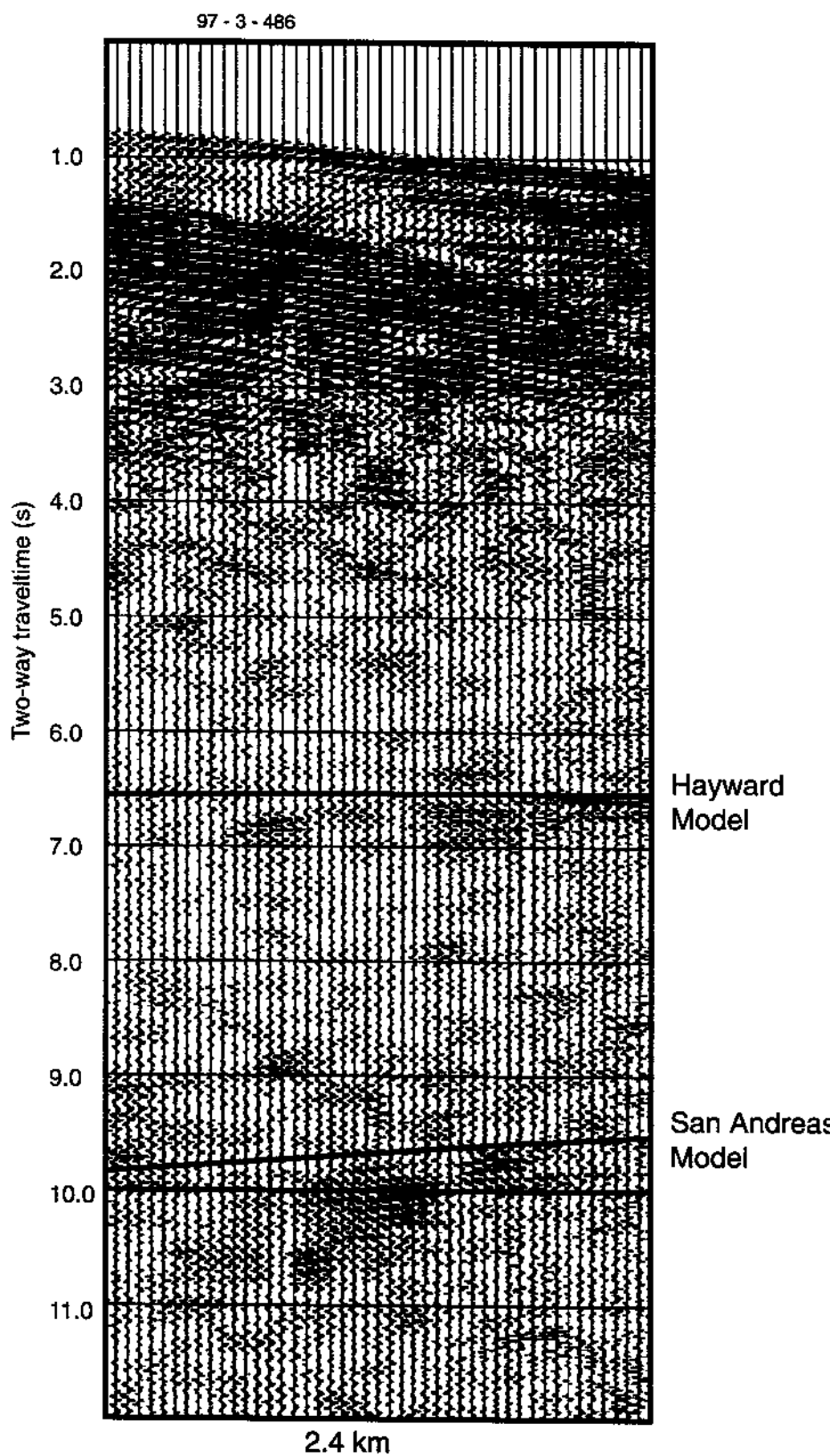


Figure 23

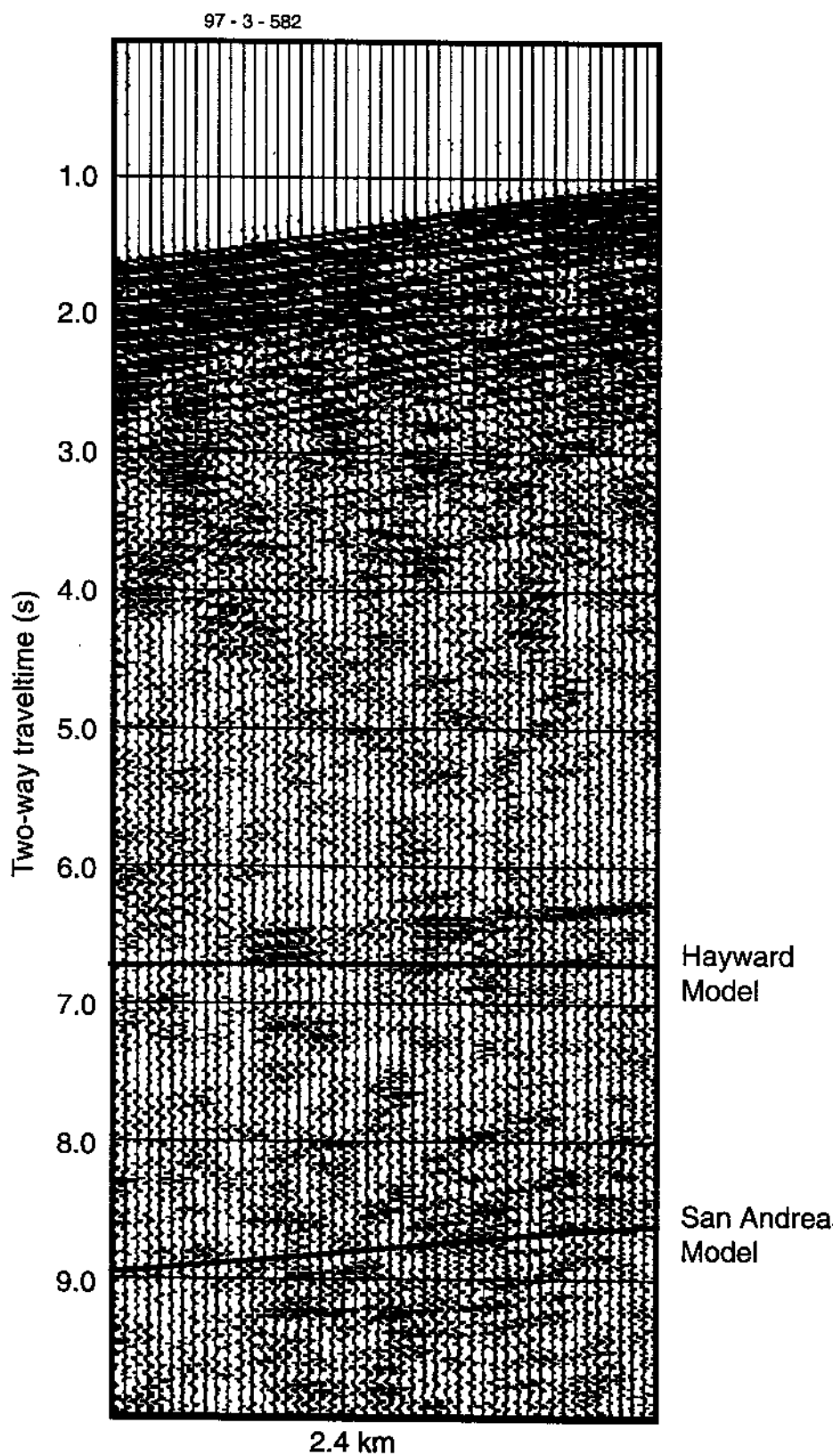


Figure 24

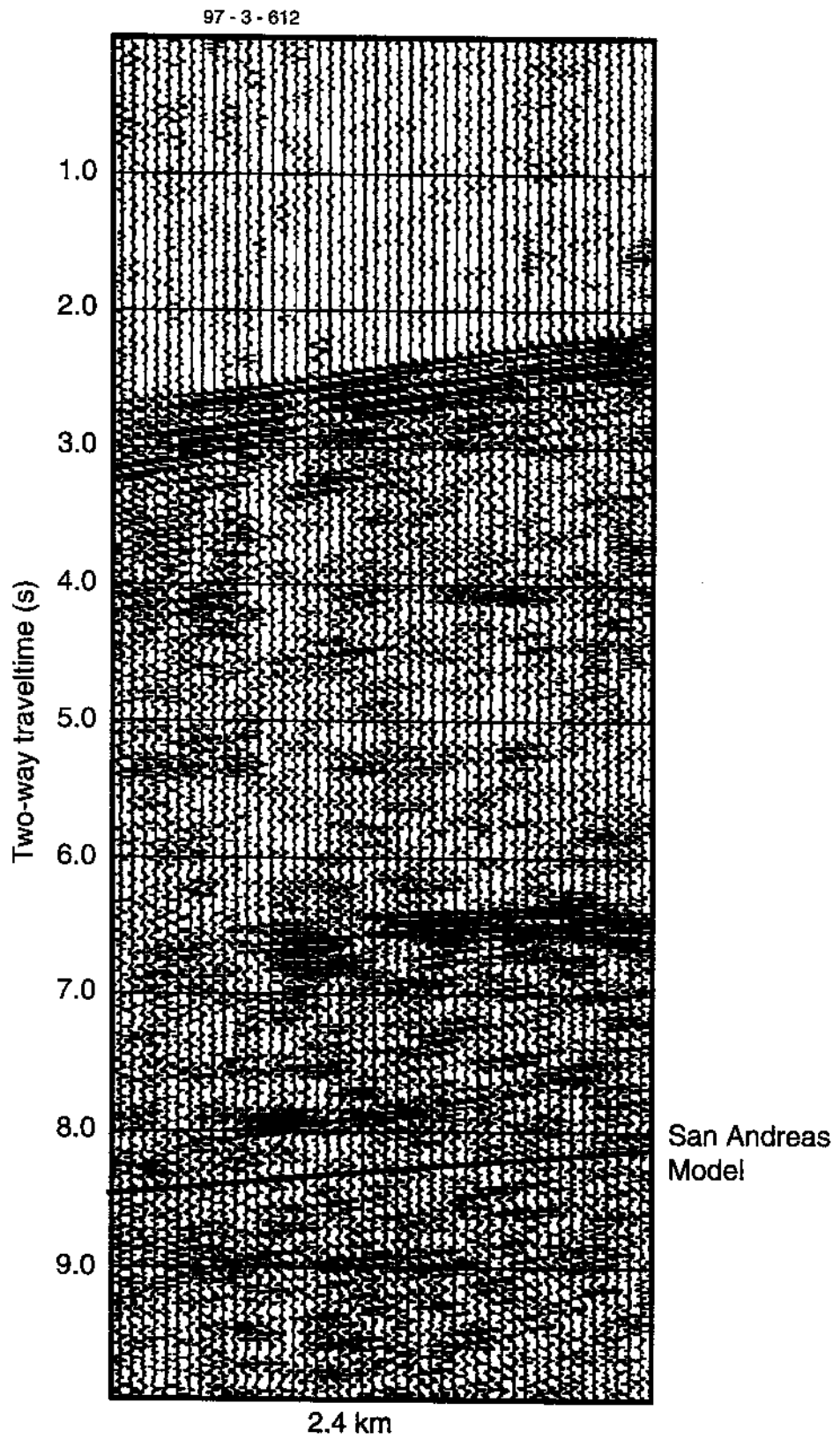


Figure 25

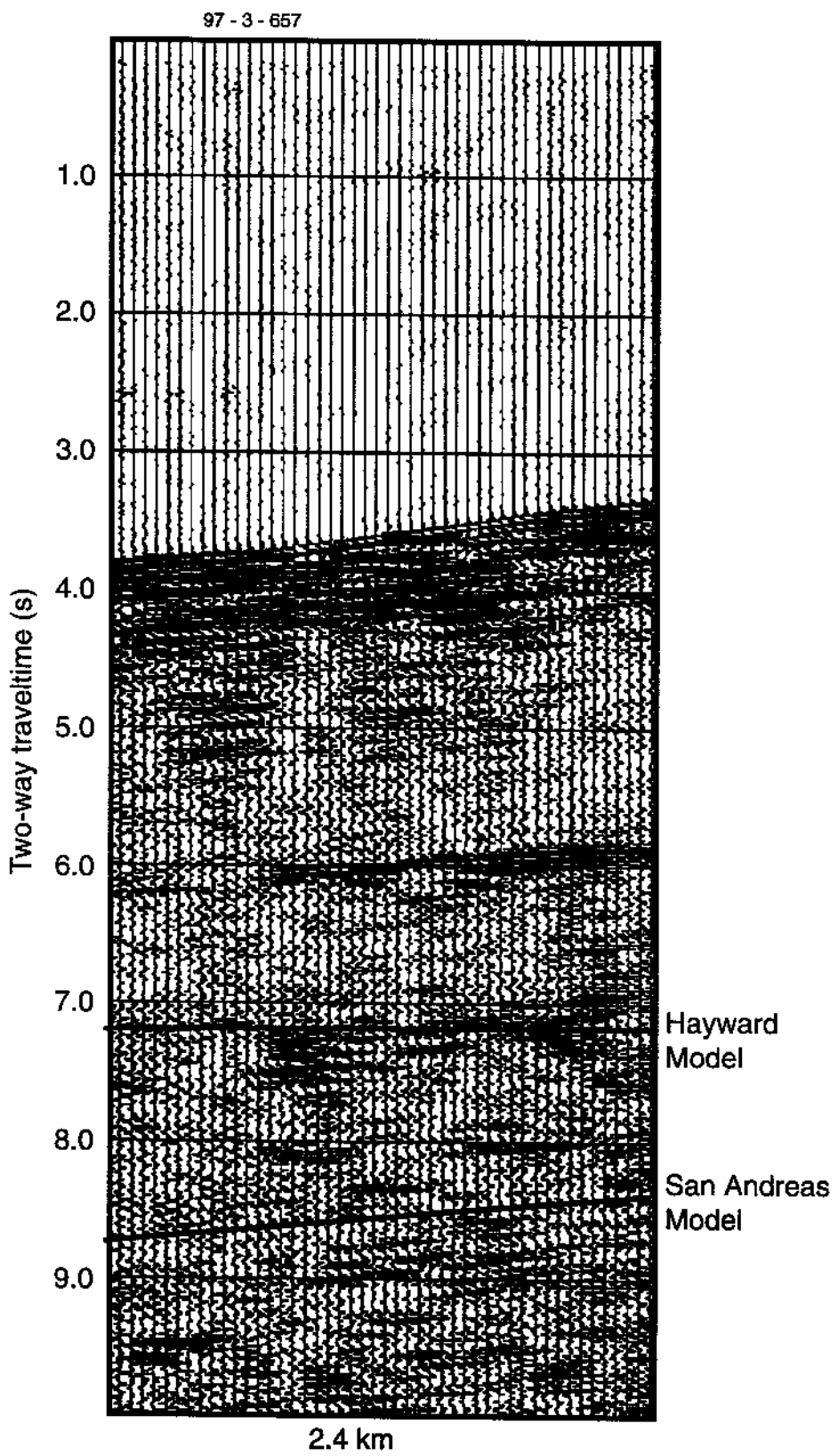


Figure 26

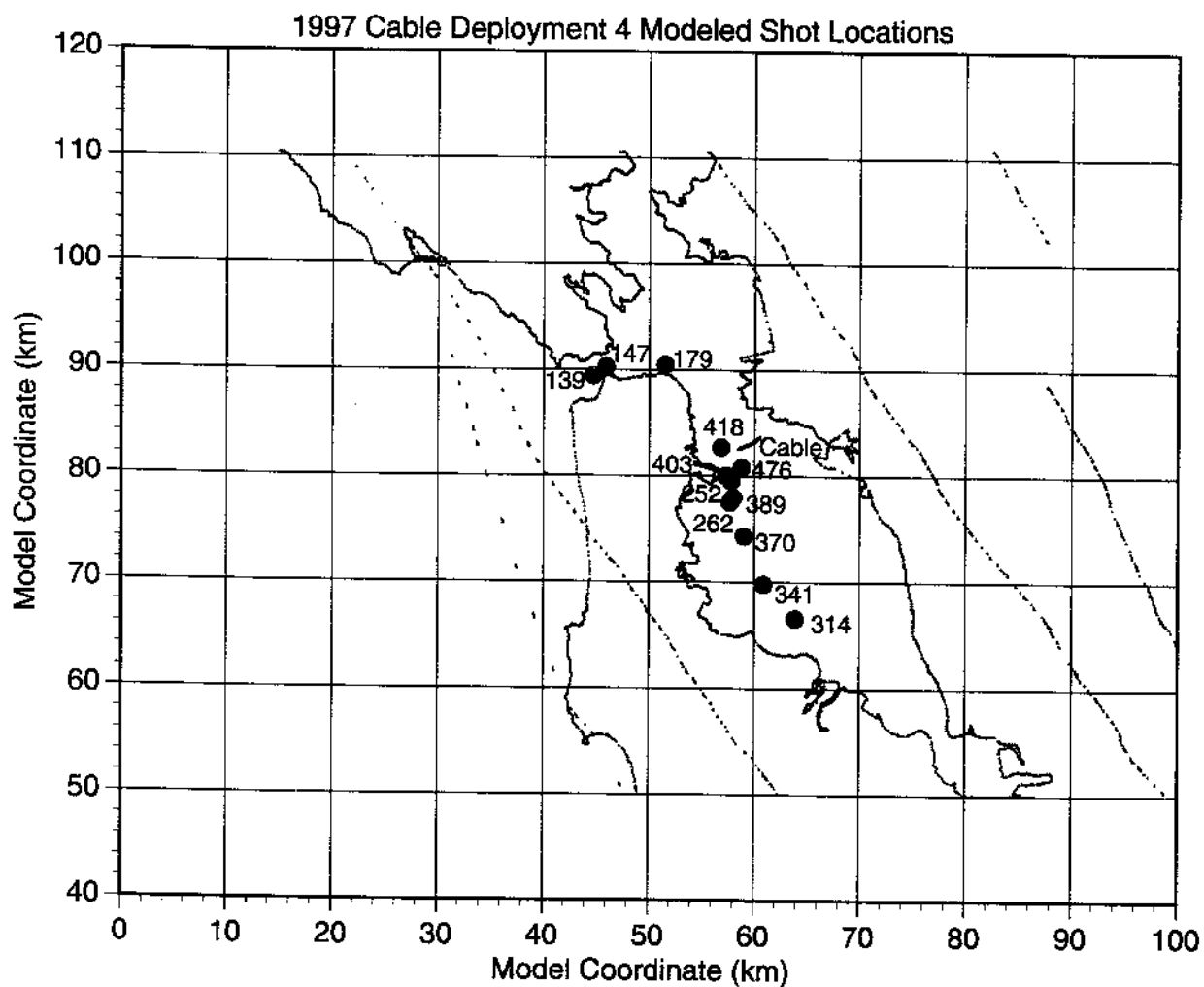


Figure 27

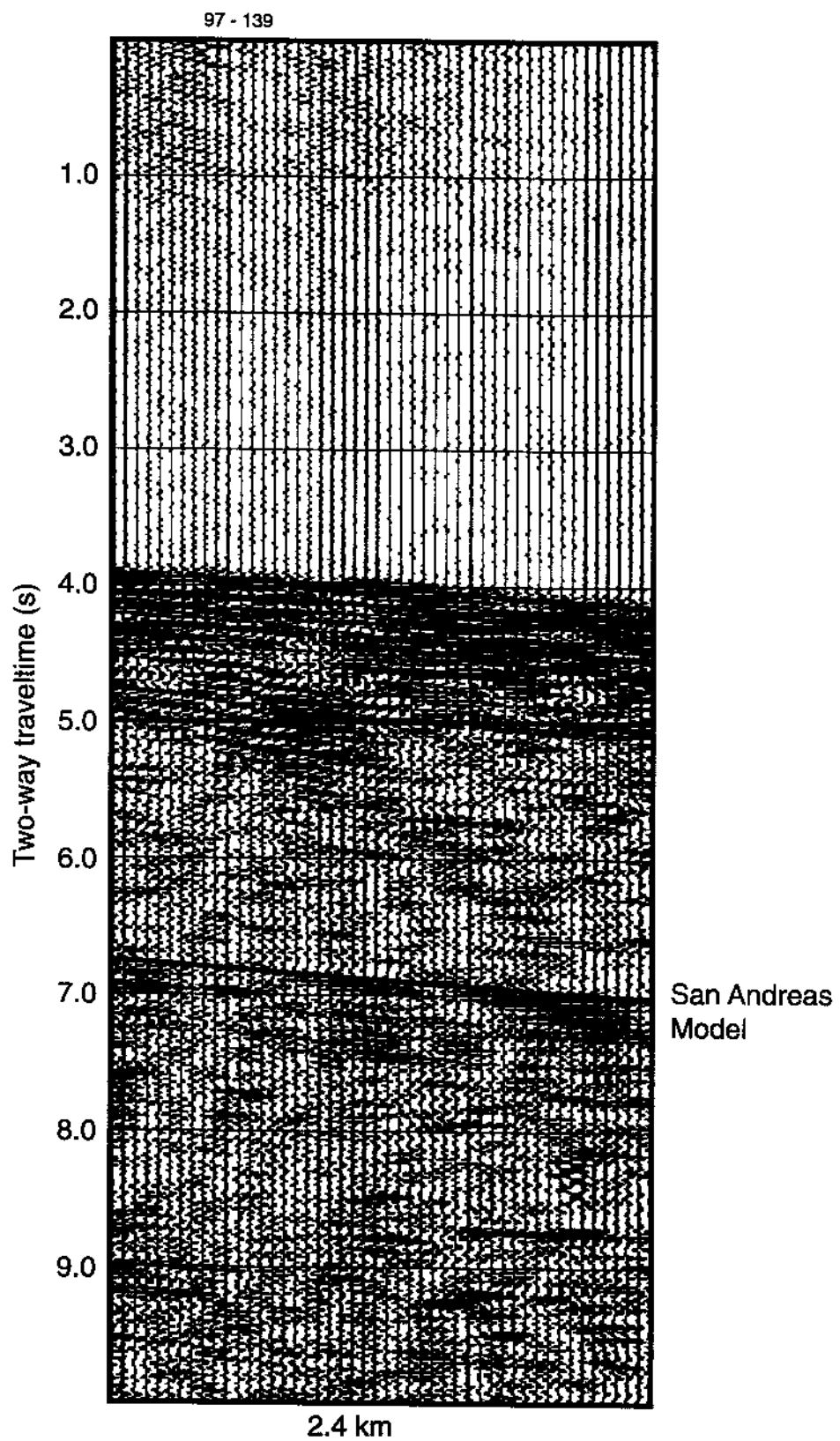


Figure 28

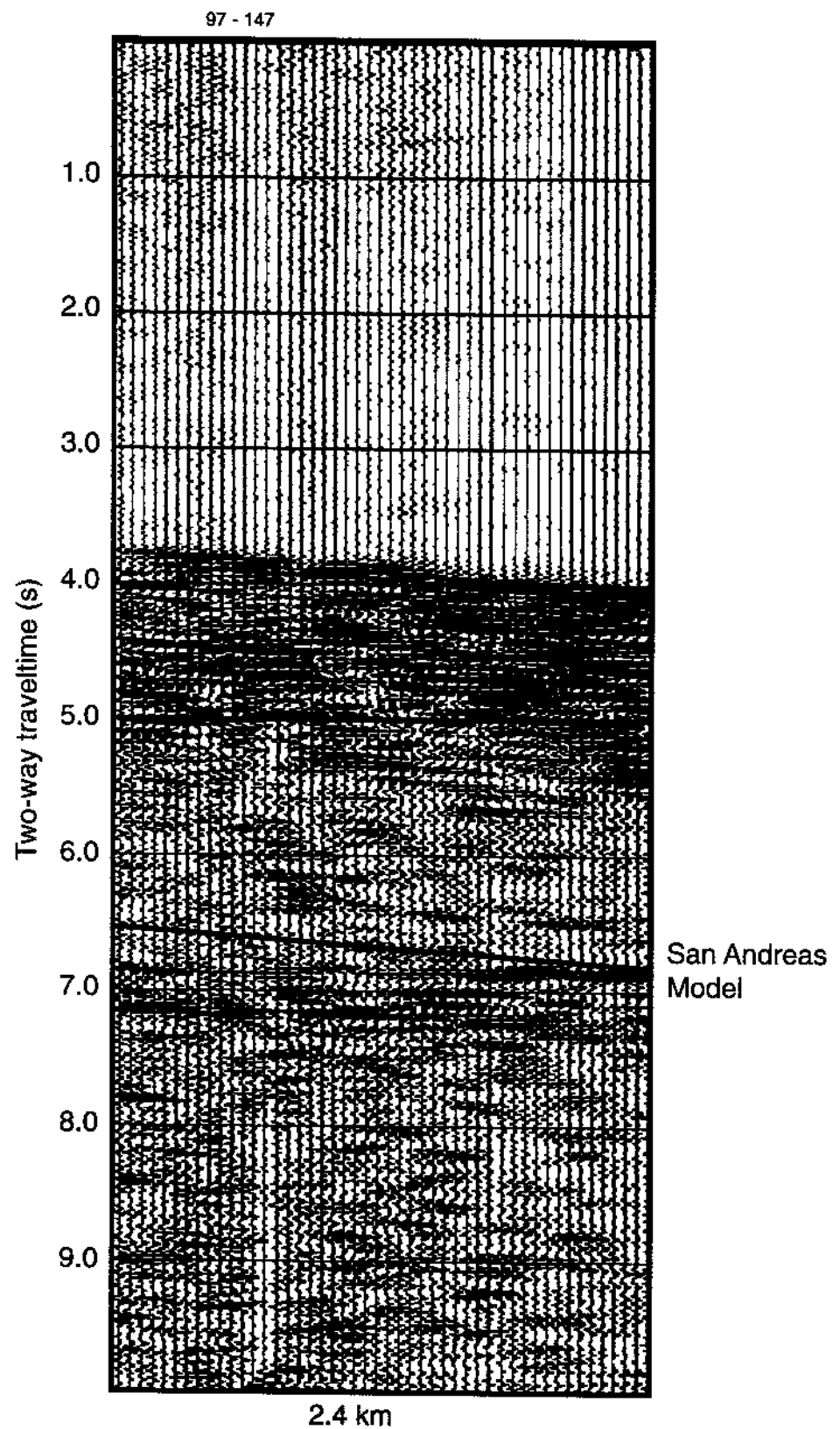


Figure 29

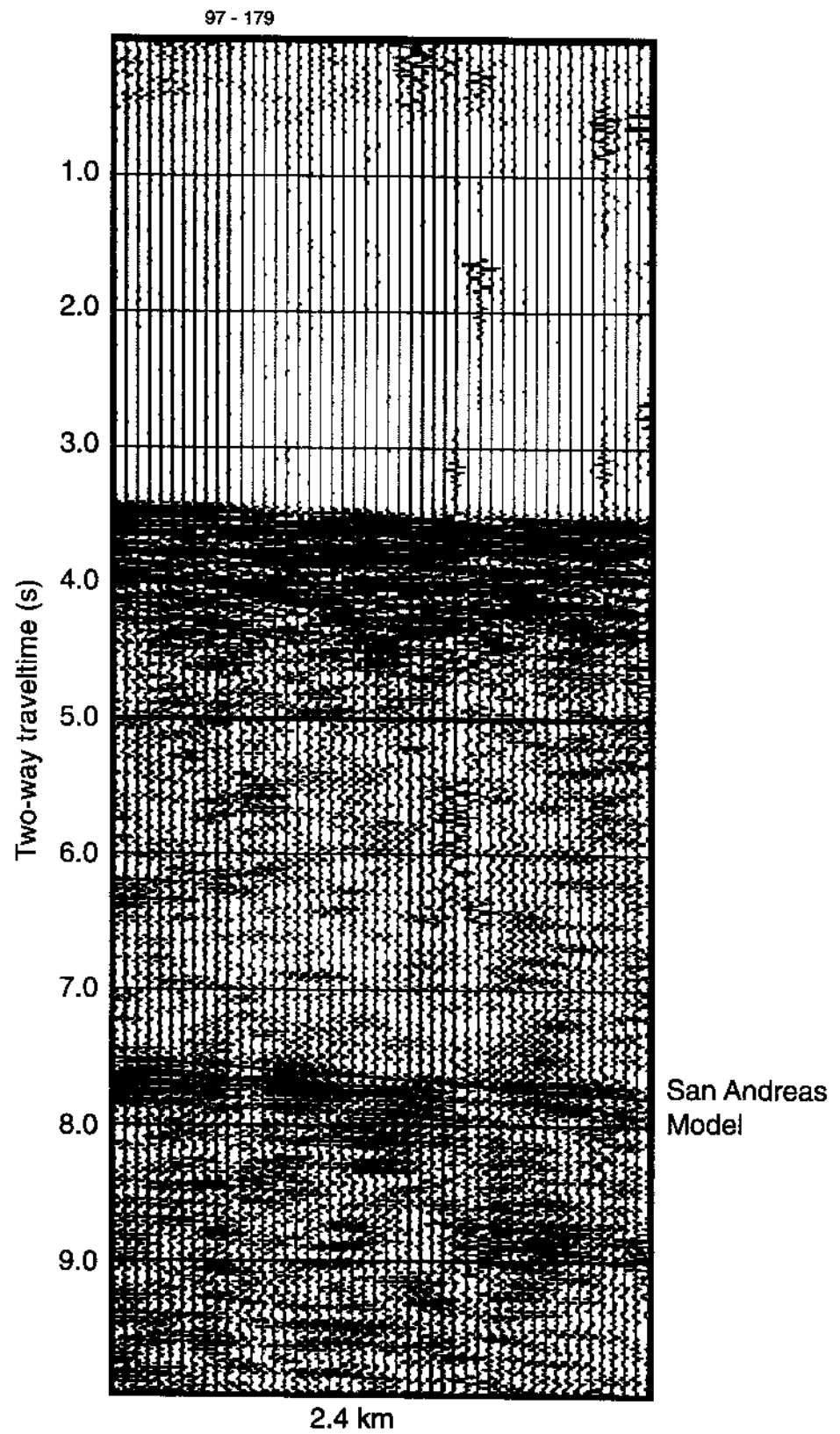


Figure 30

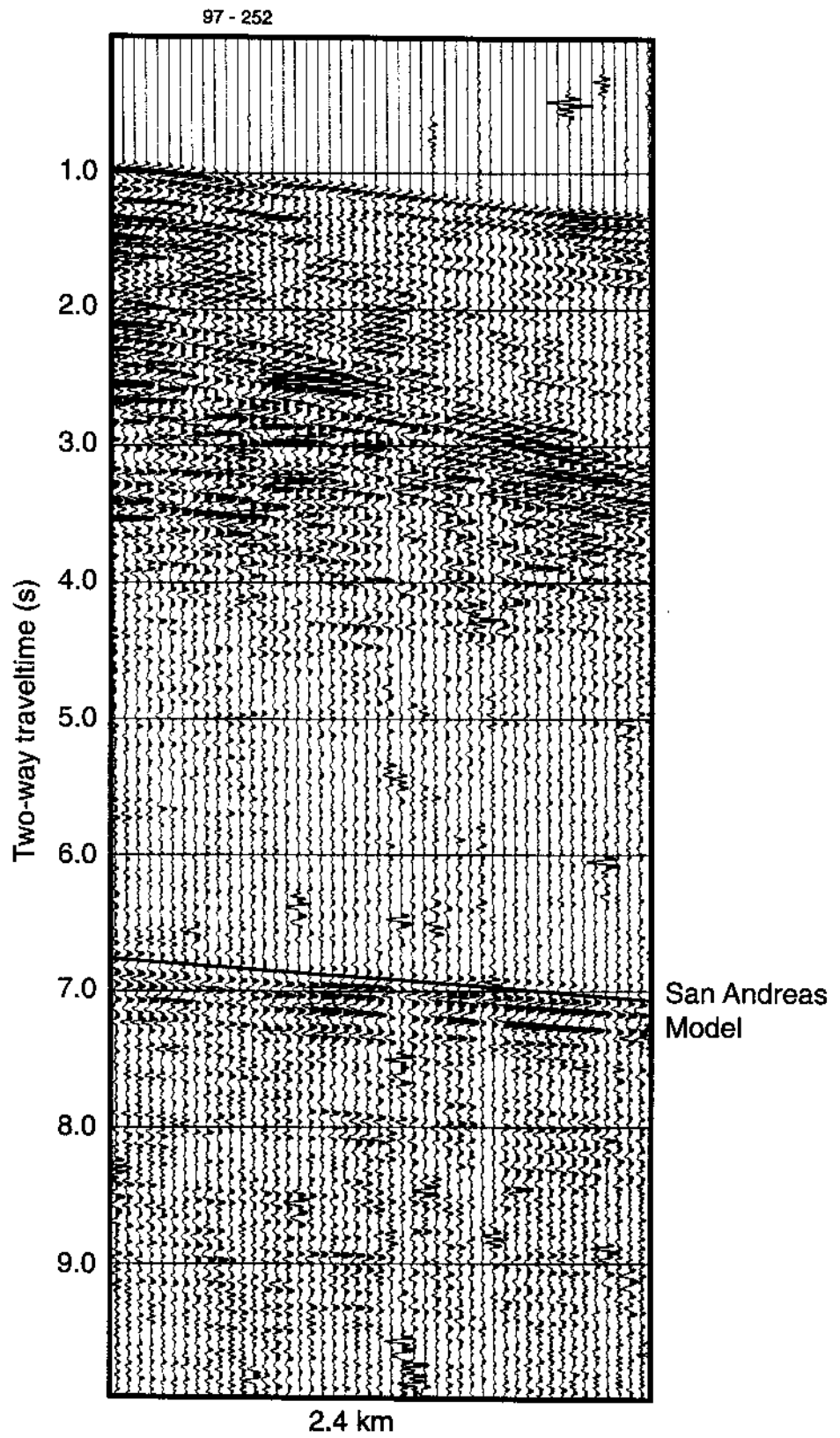


Figure 31

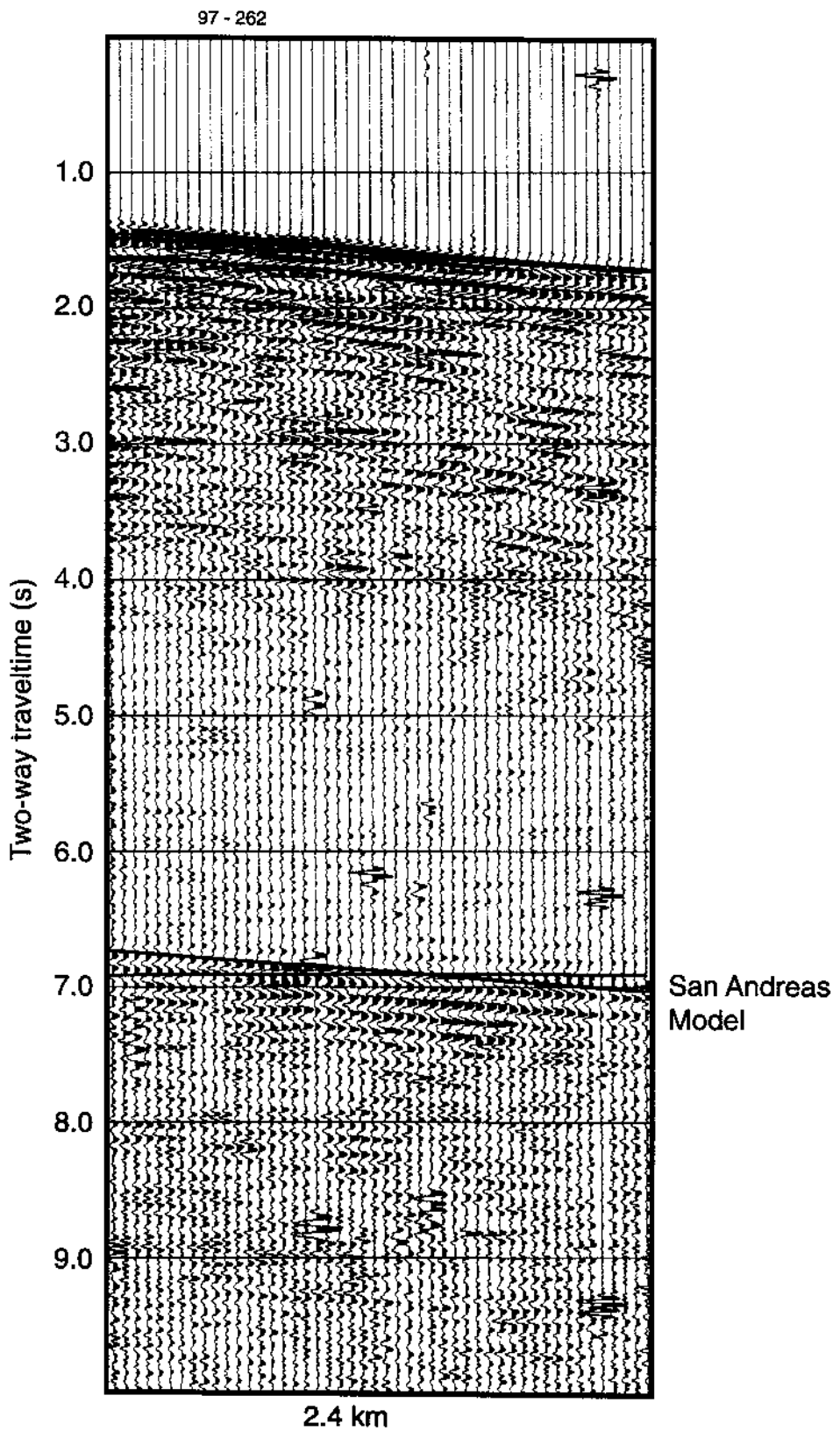


Figure 32

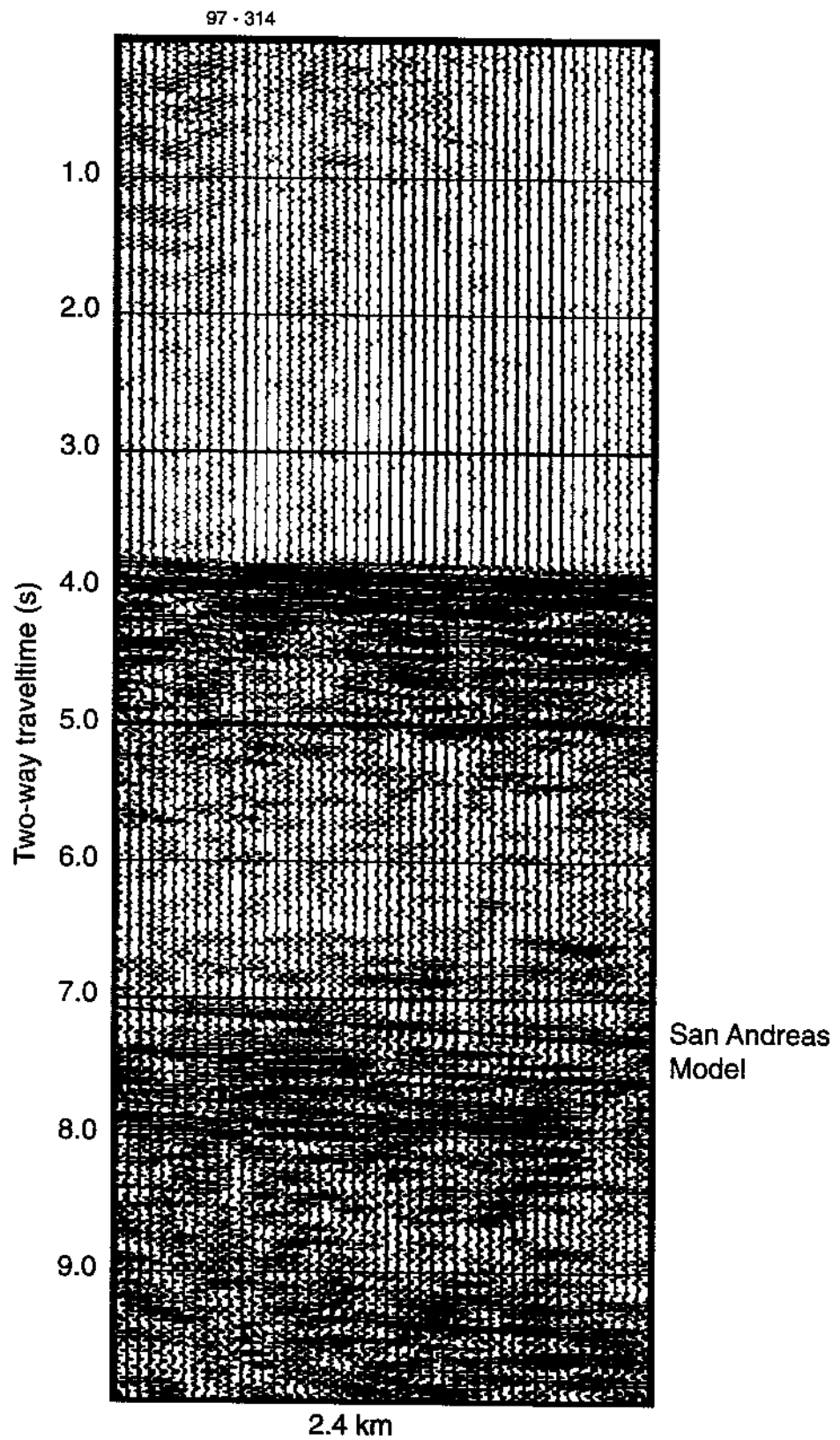


Figure 33

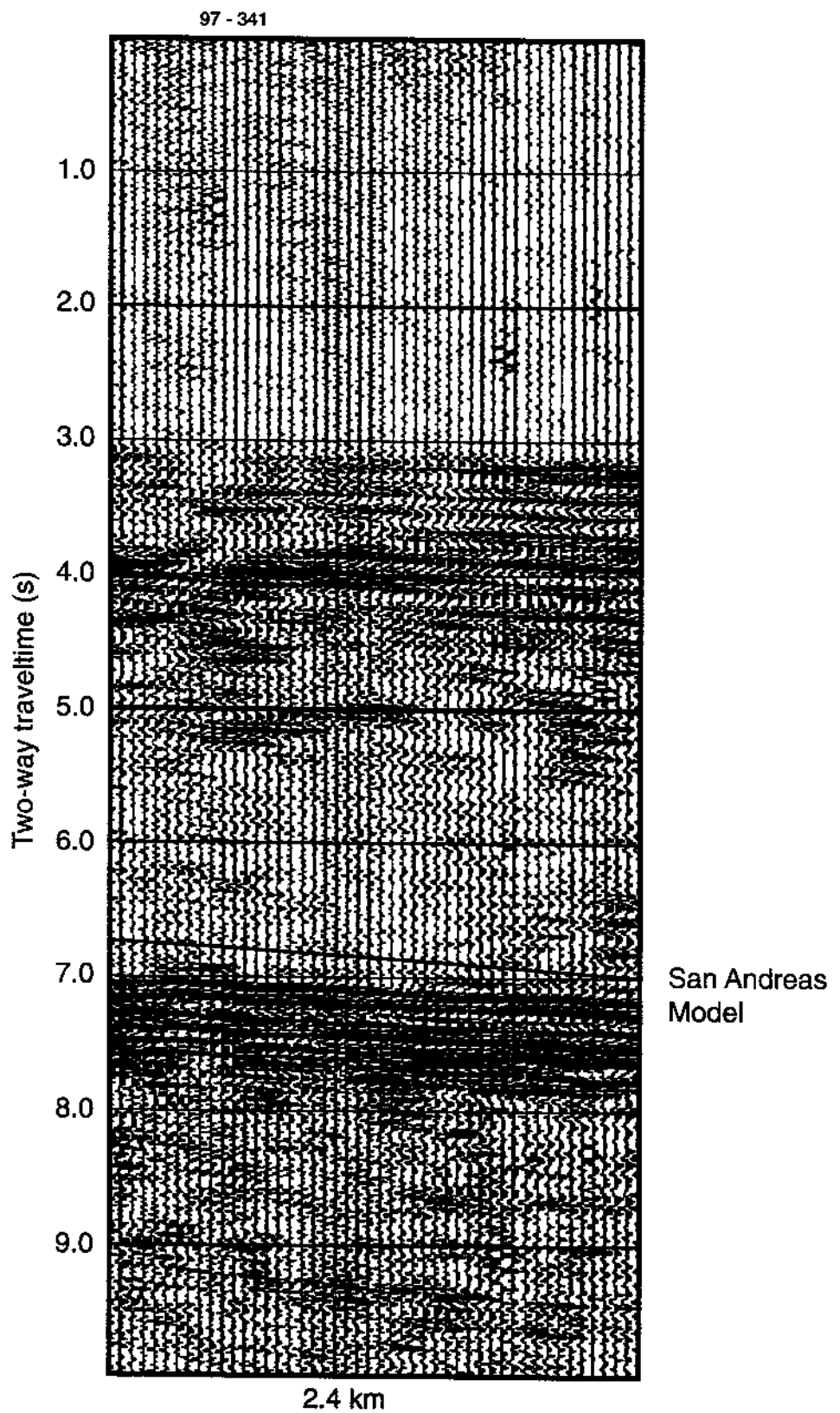


Figure 34

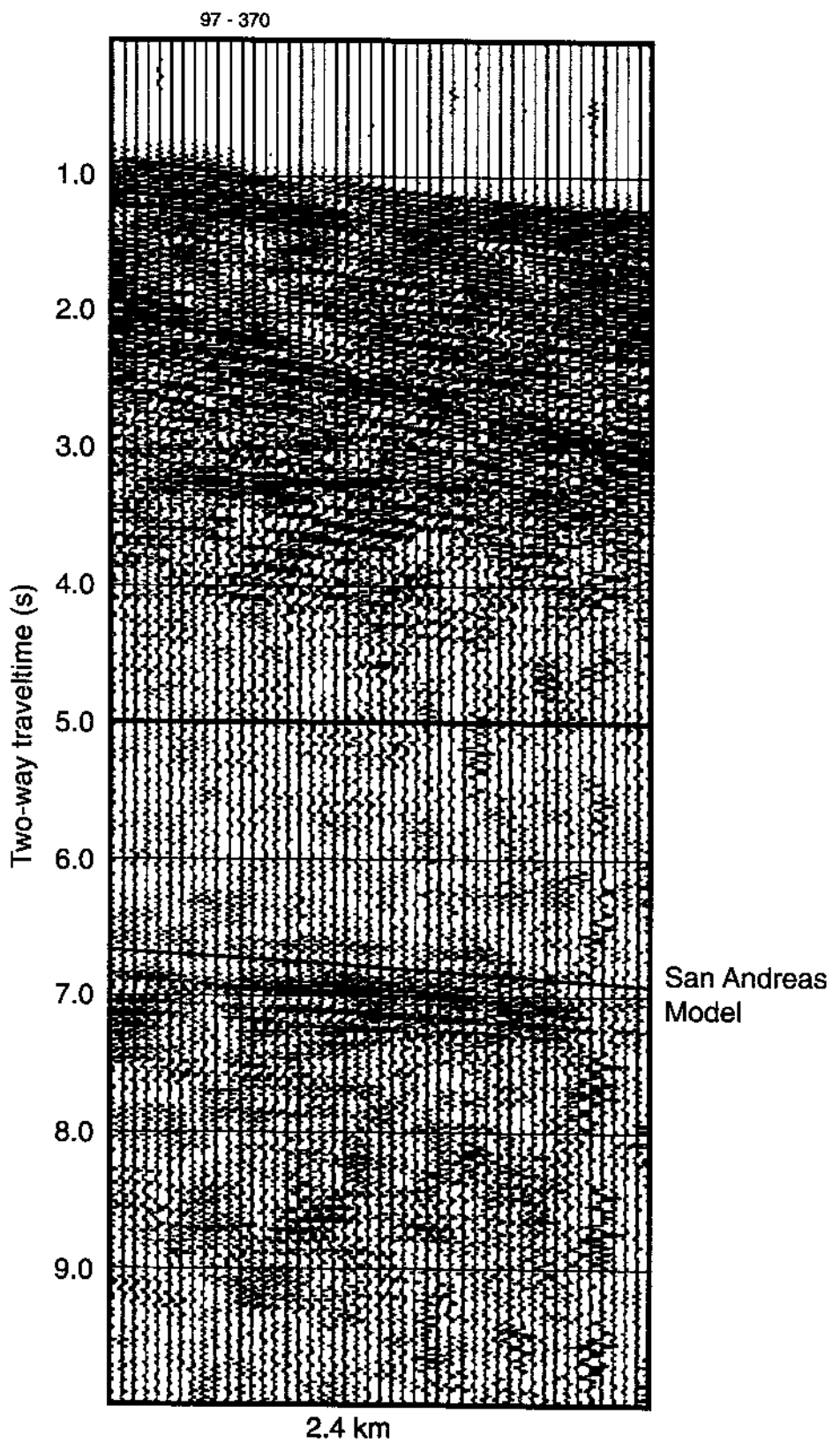


Figure 35

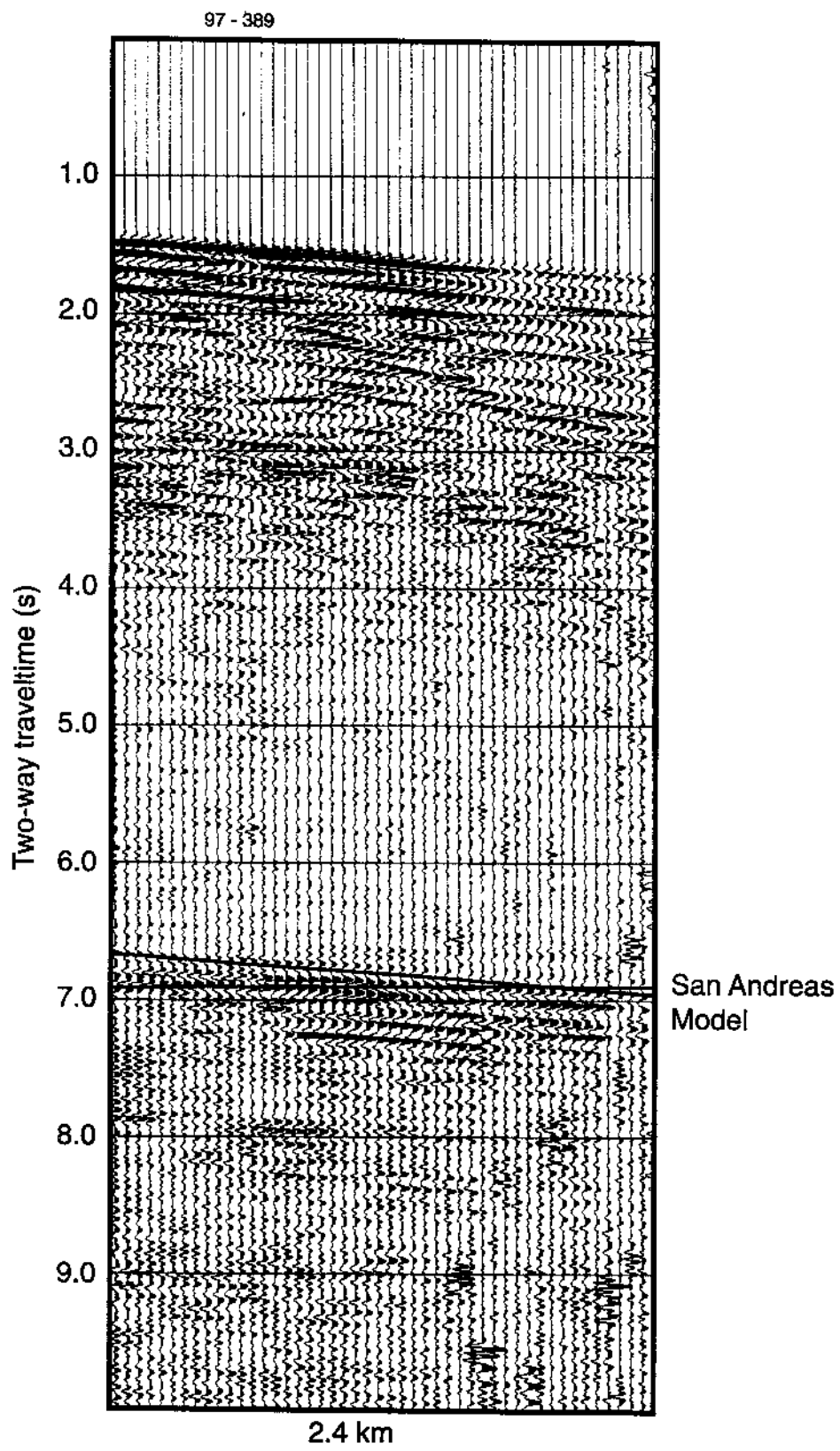


Figure 36

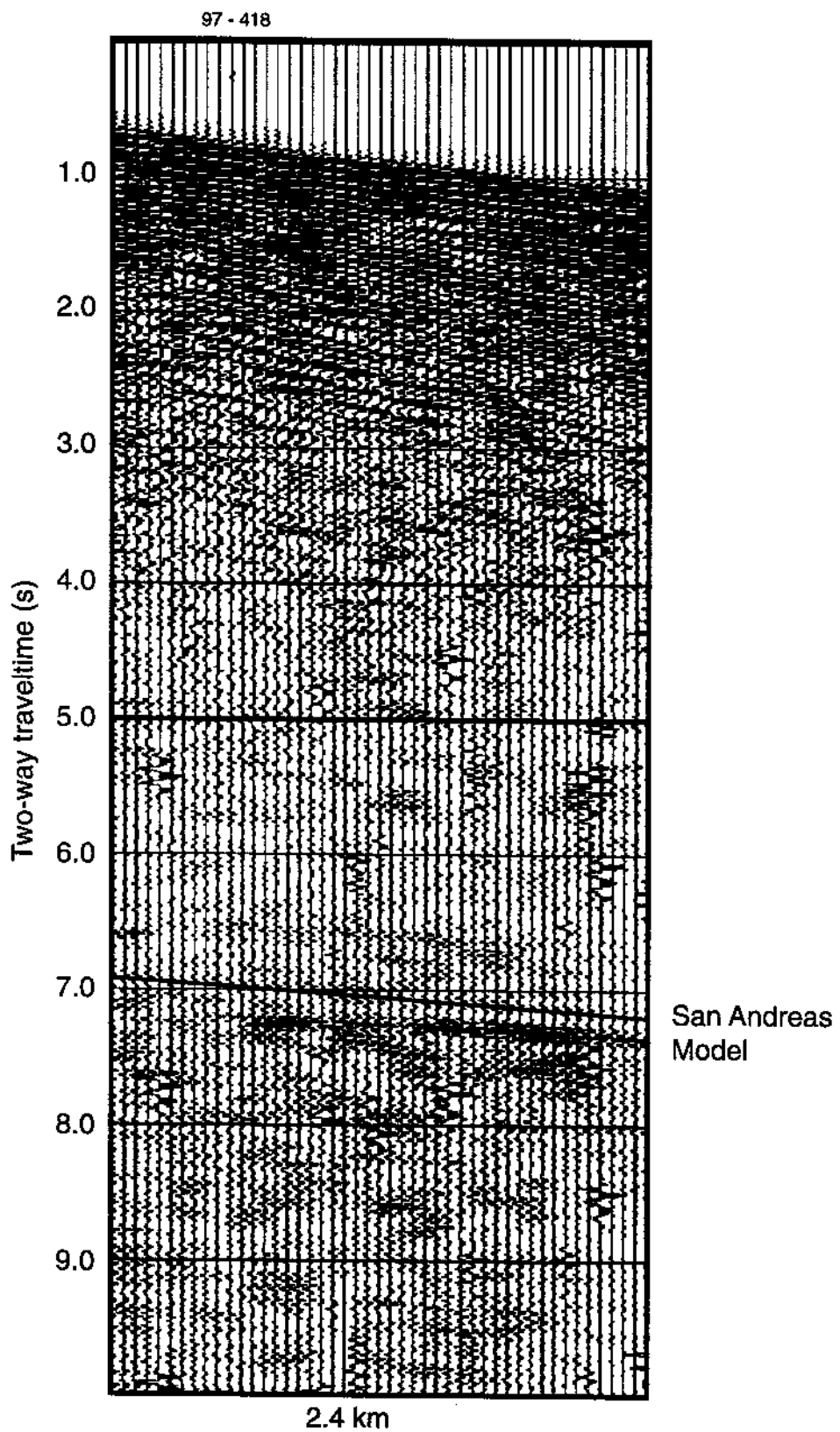


Figure 37

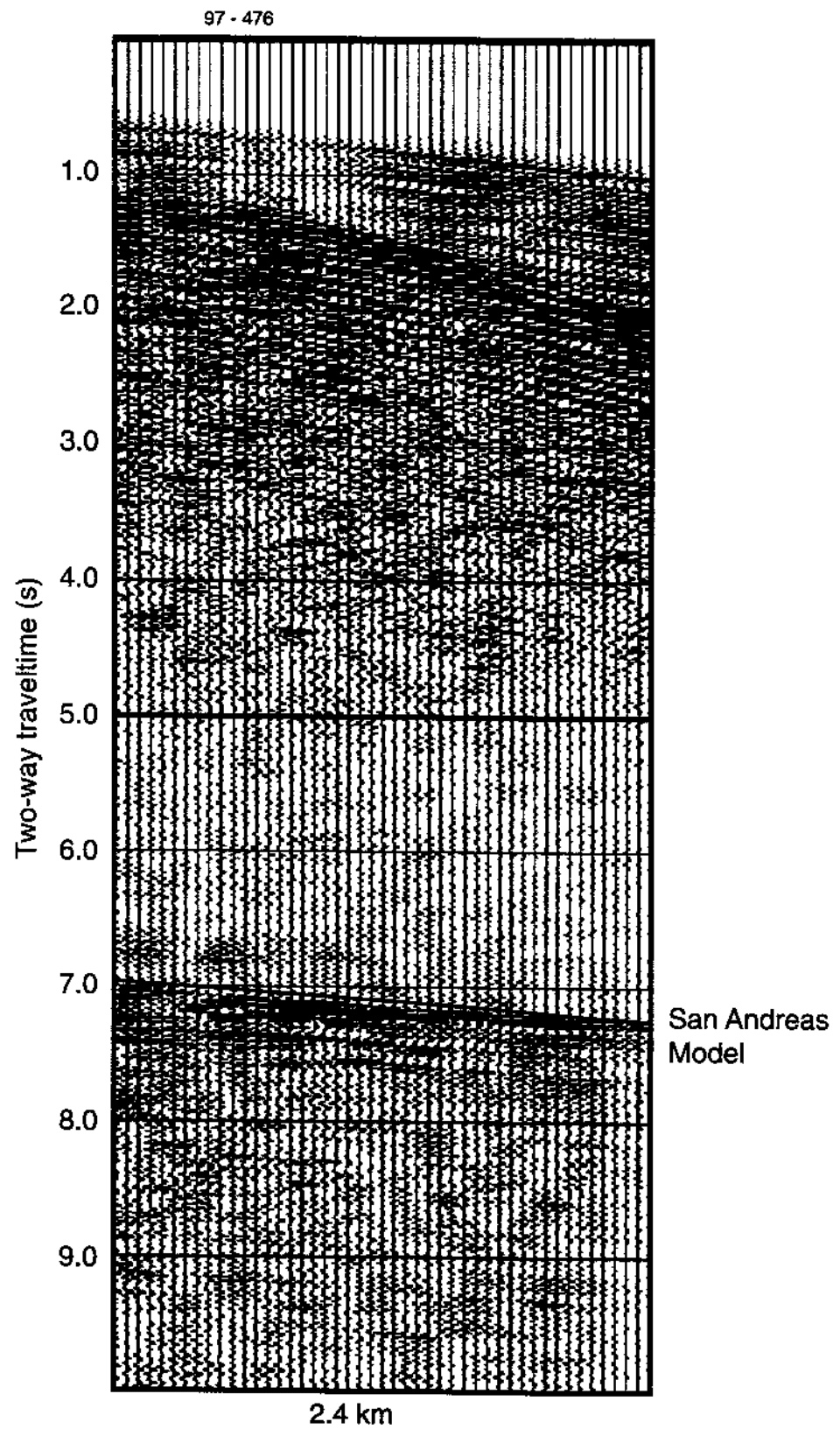


Figure 38

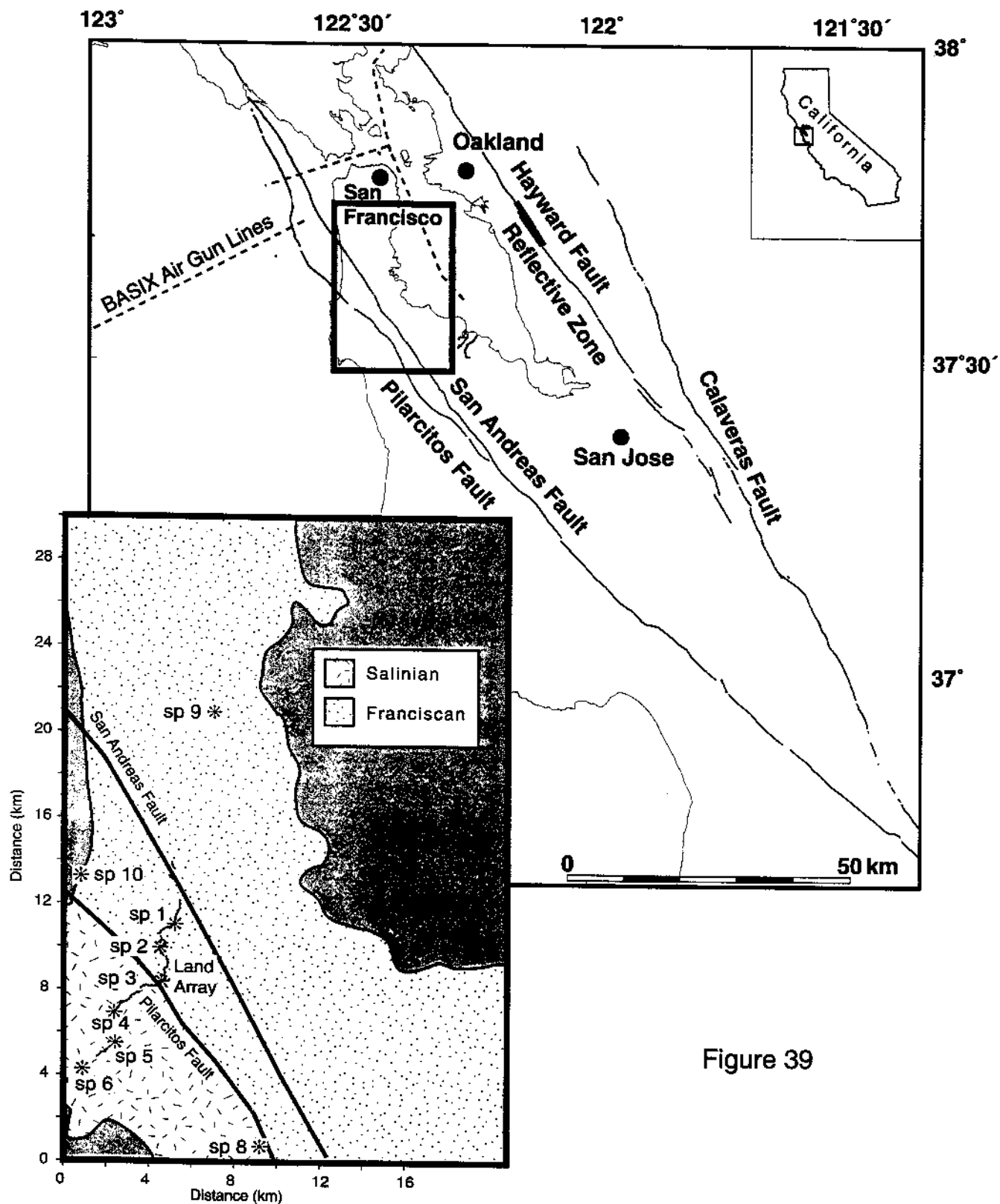


Figure 39

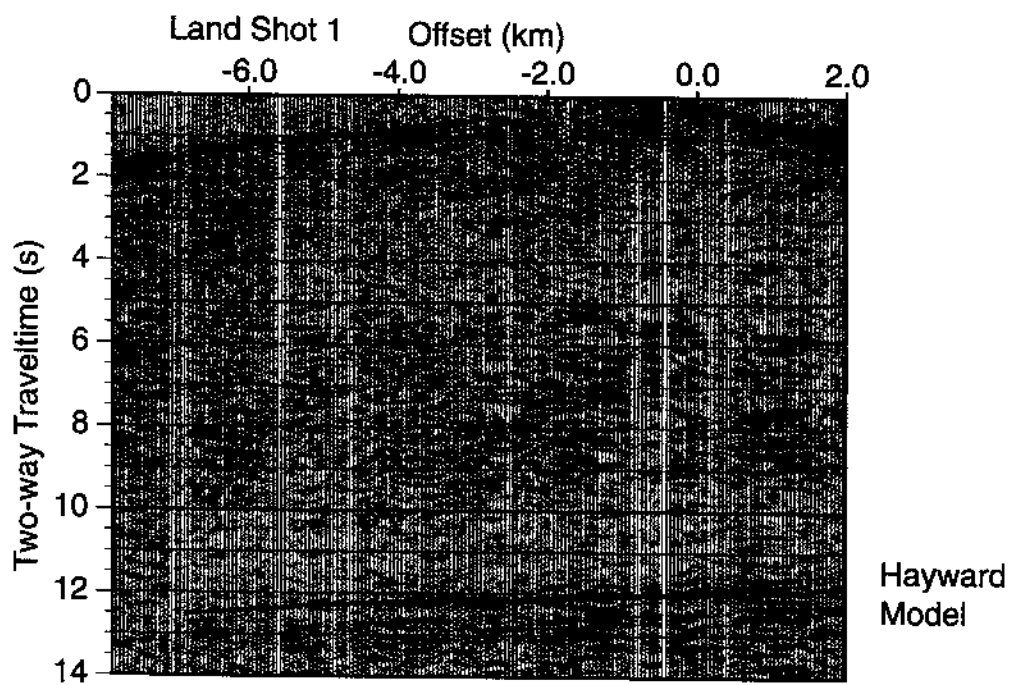


Figure 40

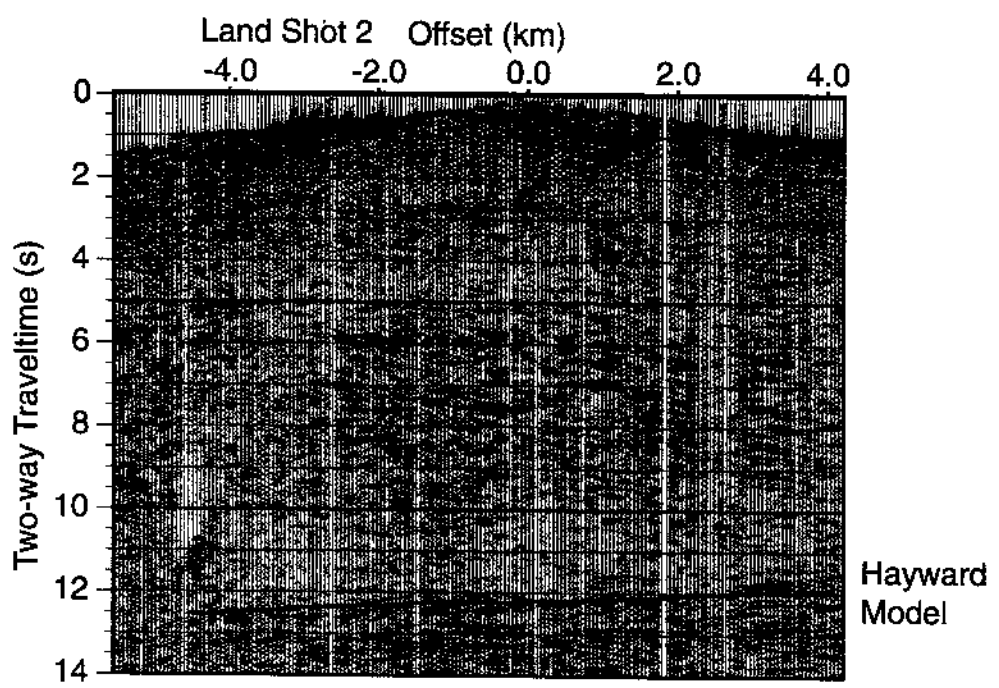


Figure 41

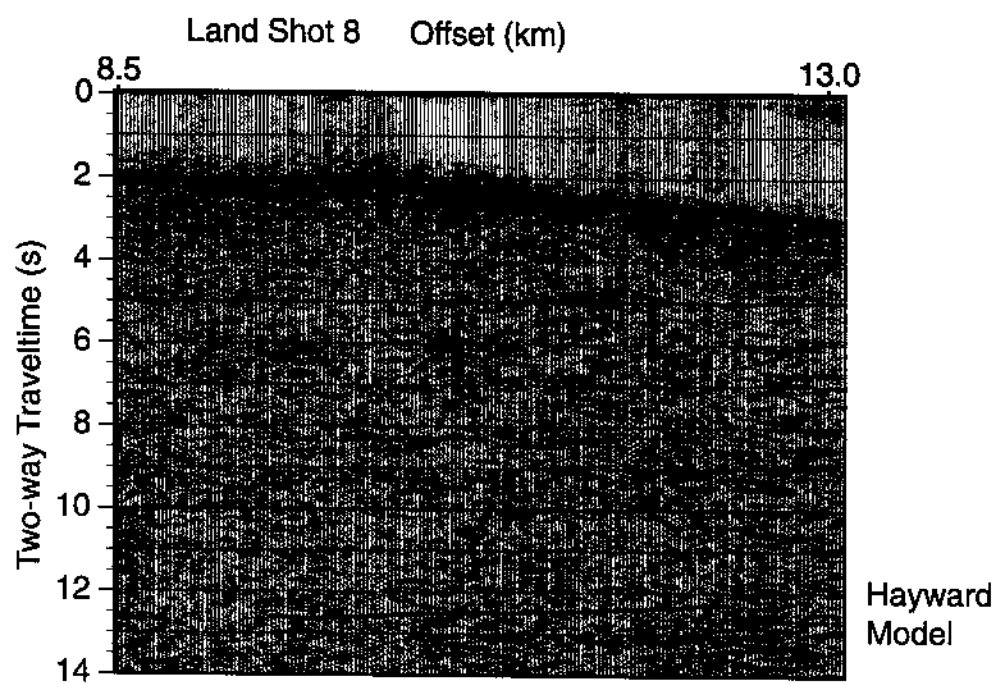


Figure 42

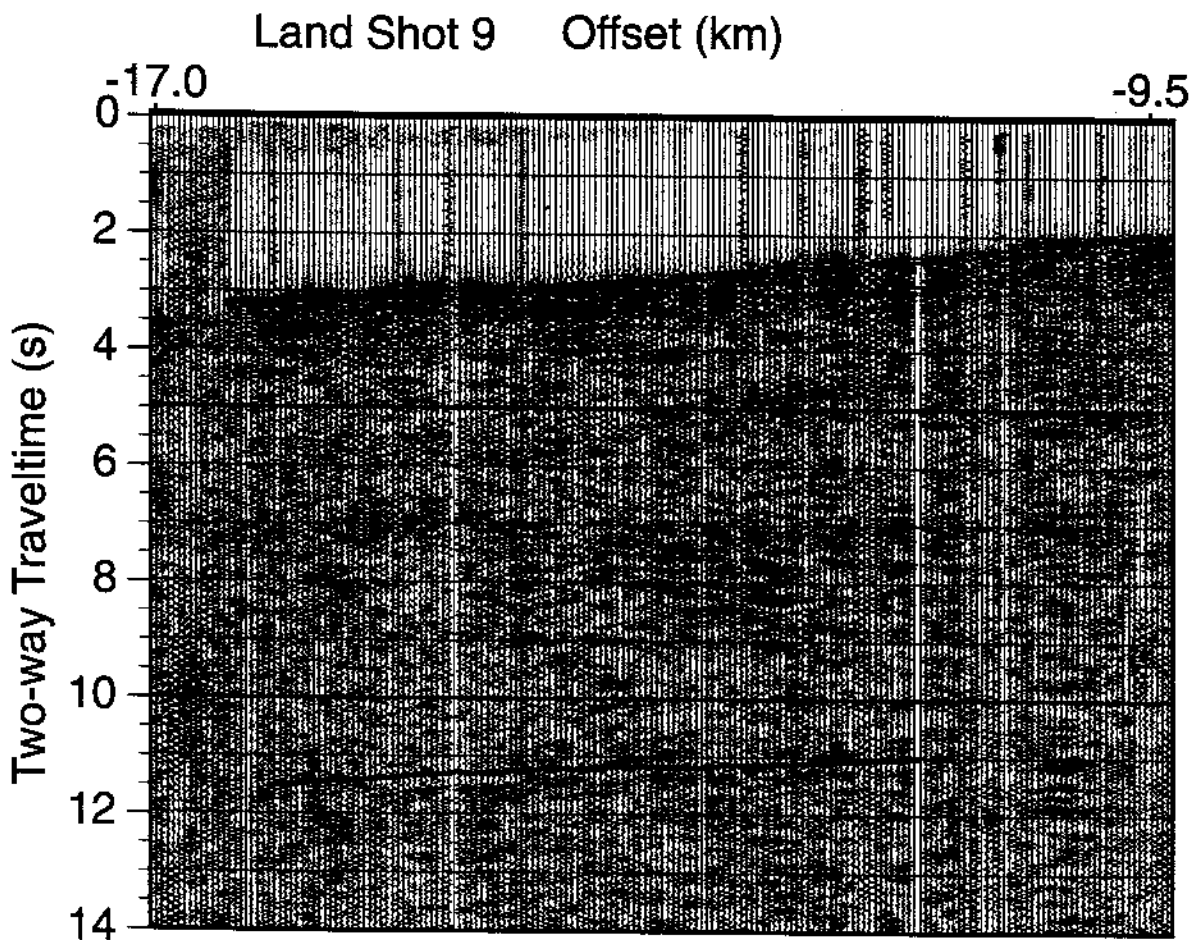


Figure 43

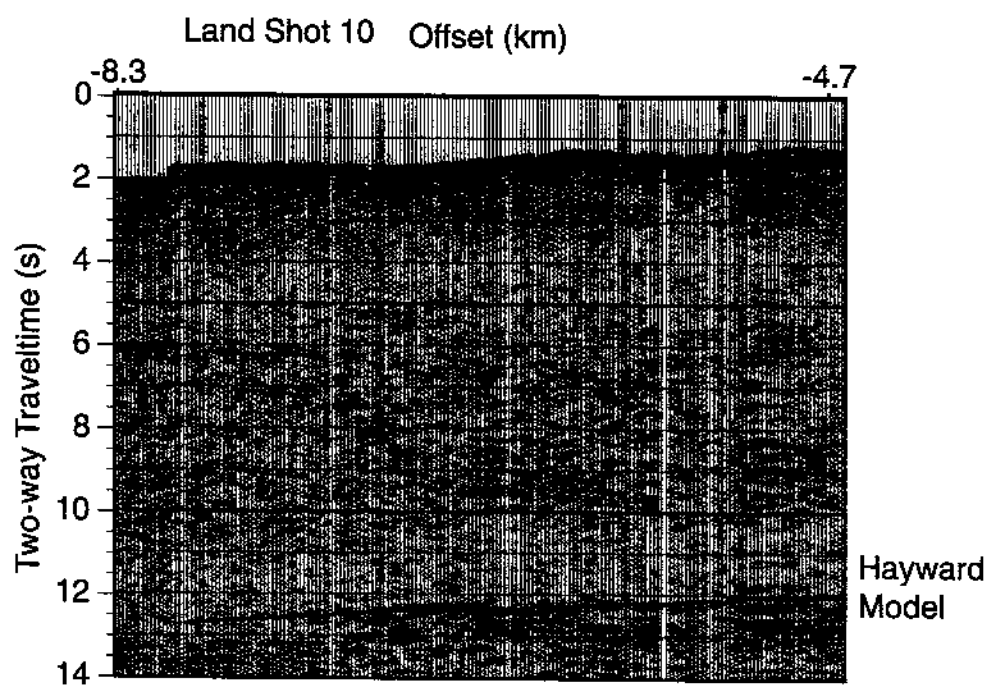


Figure 44